Challenge Journal of
CONCRETE RESEARCH LETTERS

Vol.10 No.4 (2019)

CFRP acidic environment acoustic emission
compressive strength concrete
corrosion cracking curing ductility
durability energy absorption ferrocement
flaky aggregate fly ash fracture mortar
palm oil fuel ash reinforced concrete
self-compacting concrete silica fume steel
fibers strength superplasticizer water
absorption water-cement ratio w ility

TULPAR
ACADEMIC PUBLISHING

ISSN 2548-0928

Challenge Journal of Concrete Research Letters

EDITOR IN CHIEF

Prof. Dr. Mohamed Abdelkader ISMAIL	*Miami College of Henan University, China*

EDITORIAL BOARD

Prof. Dr. Abdullah SAAND	*Quaid-e-Awam University of Engineering, Pakistan*
Prof. Dr. Alexander-Dimitrios George TSONOS	*Aristotle University of Thessaloniki, Greece*
Prof. Dr. Ashraf Ragab MOHAMED	*Alexandria University, Egypt*
Prof. Dr. Ayman NASSIF	*University of Portsmouth, United Kingdom*
Prof. Dr. Gamal Elsayed ABDELAZIZ	*Benha University, Egypt*
Prof. Dr. Han Seung LEE	*Hanyang University, Republic of Korea*
Prof. Dr. Zubair AHMED	*Mehran University, Pakistan*
Prof. Dr. Jiwei CAI	*Henan University, China*
Dr. Aamer Rafique BHUTTA	*Universiti Teknologi Malaysia, Malaysia*
Dr. Khairunisa MUTHUSAMY	*Universiti Malaysia Pahang, Malaysia*
Dr. Mahmoud SAYED AHMED	*Ryerson University, Canada*
Dr. Jitendra Kumar SINGH	*Hanyang University, Republic of Korea*
Dr. Meral OLTULU	*Atatürk University, Turkey*
Dr. Saleh Omar BAMAGA	*University of Bisha, Saudi Arabia*

E-mail: *cjcrl@challengejournal.com*

Web page: *cjcrl.challengejournal.com*

TULPAR Academic Publishing
www.tulparpublishing.com

Challenge Journal of Concrete Research Letters

CONTENTS

Research Articles

Challenge Journal of Concrete Research Letters

Research Article

Multiple repair scenario of life cycle cost of RCC girder bridge using Markov chain model

Md. Shafiqul Islam [a], Shayla Sharmin [b,*], Jebunnesa Islam [a]

[a] *Department of Civil Engineering, Rajshahi University of Engineering & Technology, Kazla 6204, Rajshahi, Bangladesh*
[b] *Department of Building Engineering and Construction Management, Rajshahi University of Engineering & Technology, Kazla 6204, Rajshahi, Bangladesh*

ABSTRACT

At present, many road authorities in the world face challenges in condition monitoring diagnosis of distress and forecasting deterioration, strengthening and convalescence of aging bridge structures. The accurate prediction of the future condition is crucial for optimizing the maintenance activities. It is very tough to predict the actual performance scenario or actual in–situ structures without carrying out inspection. Limited availability of detailed inspection data is considered as one of the major drawbacks in developing deterioration models. In State Based Markov deterioration (SNMD) modelling, the main job is to estimate transition probability matrixes (TPMs). In this paper, Markov Chain Monte Carlo (MCMC) is used to estimate TPMs. In Markov Chain Model, future conditions depend on only present bridge inspection data. Multiple repair options are adopted in order to optimize life cycle cost. Repairs are needed when the critical chloride concentration exceeds 0.2. Three distinct types of cost corresponding to each repair option is considered. The objective of this paper is to minimize the life cycle cost considering appropriate repair timings of mixed repair methods. Variation of life cycle cost of five different concretes (stronger to weaker) using three different repair option is shown in this paper. For specific normalized condition of concrete's failure probability (0.3) and specific type of concrete, variation of life cycle cost using multiple repair options is also shown in this paper.

ARTICLE INFO

Article history:
Received 26 August 2019
Revised 19 November 2019
Accepted 24 November 2019

Keywords:
Monte Carlo simulation
Markov chain
Transition probability matrix
Repair matrix

1. Introduction

Various random impact factors can initiate time dependent deterioration in RCC Girder Bridge. They can vary in loading and environmental conditions. In Girder Bridge, girders are used to support the deck. Girders are made of concrete which is deteriorated by increasing chloride concentration. It is an important factor for bridge deterioration. Chloride can come into water from various wastes, which causes corrosion in reinforced concrete structure. The corrosion occurred when the ion chloride has reached the steel reinforcement and the corrosion has begun to spread which caused spalling on concrete cover. As a result chloride penetration often causes failure of structure before the lifetime service of structure. It also reduces the compressive strength and accelerates the corrosion of reinforcement bars in recycled aggregate concrete. Nowadays, it is essential to establish an effective maintenance and repair strategy to keep bridges sufficiently safe and serviceable throughout their service lives. To prevent shortened structure lifetime the initiation time of chloride penetration must be delayed.

2. Modelling of Bridge Deterioration

Bridge deterioration is the process of declining in the condition of bridge resulting from normal operating conditions. The deterioration process exhibits the complex phenomena of physical and chemical changes that occur in different bridge components. Generally, deterioration models can be categorized into three categories. They are: deterministic models, stochastic models, and artificial intelligence models. These categories are discussed below.

* *Corresponding author*. Tel.: +880-17-5447-2244 ; E-mail address: shaylasharmin.100016@gmail.com (S. Sharmin)
ISSN: 2548-0928 / DOI: https://doi.org/10.20528/cjcrl.2019.04.001

a) Deterministic Models

These models calculate the predicted conditions deterministically by ignoring the random error in prediction. These models can be used for analysis of networks with a large population. However, they are considered to have some drawbacks:

i) The current condition and the condition history of individual facilities are not considered while predicting the average condition of a family of facilities (Shahin et al., 1987; Jiang and Sinha, 1989)

ii) They estimate facility deterioration for the "no maintenance" strategy only because of the difficulty of estimating the impacts of various maintenance strategies (Sanders and Zhang, 1994)

iii) Updating these models with new data is very tough

b) Stochastic Models

The uncertainty and randomness of facility deterioration process are considered as one or more random variables in stochastic models. Among the stochastic techniques Markovian models has been used extensively in modelling the deterioration of infrastructure facilities (Butt et al., 1987; Jiang et al., 1988). These models use the Markov Decision Process (MDP) to determine the expected failure condition of facility based on previous condition. The uncertainty of the deterioration process and considering the current facility condition in predicting future one, these two problems of deterministic models have been covered by Markovian models. In this study, stochastic models are used to predict future condition.

c) Artificial Intelligence (AI) Models

These models make use of computer techniques that aim to automate intelligent behaviors. Artificial neural networks (ANN), genetic algorithm (GA), and case based monitoring (CBR) are used to optimize the future prediction conditions. Sobanjo (1997) has performed detailed investigation to use the ANN in modelling bridge deterioration. Even though ANN has automated the process of finding the polynomial that best fits a set of data points, it still shares the problems of the deterministic model.

3. Prediction of Performance by Markov Chain Models

3.1. Markov chain

A Markov chain is a mathematical model of a random phenomenon evolving with time in a way that the past affects the future only through the present. The "time" can be discrete (i.e. the integers), continuous (i.e. the real numbers), or, more generally, a totally ordered set. Markov chain is the distinctive case of the Markov process whose development can be treated as a series of transitions between certain states. Markov process describes the probability of attaining a future state in the process which is dependent only on the present state not on the previous state.

3.2. Transition probability matrix formation

A Markov transition matrix is a square matrix describing the probabilities of moving from one state to another in a dynamic system. The rows of Markov transition matrix are valued as one. Transition probability matrix is also the matrix form of probabilities where each element denotes the transition probabilities of system having in the same state or to the higher states with time. While developing performance prediction models for bridge components Markov chains are used, which includes defining discrete condition states and accumulating the probability of transition from one condition state to another over multiple discrete time intervals. Transition probabilities are represented by a matrix of order $n \times n$ called the transition probability matrix (P), where n is the number of possible condition states. Each element (P_{ij}) in this matrix represents the probability that the condition of a bridge component will change from state (i) to state (j) during a certain time interval called the transition period, where the following relation is valid $0 \leq P_{ij} \leq 1$.

It is assumed that the transition probabilities are not time dependent (t_n, t_{n+1}). Two more conditions apply to the process when it is used to predict deterioration. Firstly, $P_{ij}=0$ for $i>j$, signifying the belief that bridges cannot improve in condition without first receiving treatment. Secondly, $P_{nn}=1$, signifying a holding state where by bridges that have reached their worst condition cannot deteriorate further. If the initial condition vector $P(0)$ that describes the present condition of a bridge component is known, the future condition vector $P(t)$ at any number of transition periods (t) can be obtained as follows (Collins, 1975):

$$P(t) = P(0) \cdot P(t) \tag{1}$$

where

$$P = \begin{bmatrix} p_{11} & p_{12} & \cdots & p_{1n} \\ p_{21} & p_{22} & \cdots & p_{2n} \\ \cdots & \cdots & \cdots & \cdots \\ \cdots & \cdots & \cdots & \cdots \\ \cdots & \cdots & \cdots & \cdots \\ p_{n1} & p_{n2} & \cdots & p_{nn} \end{bmatrix} \tag{2}$$

The values composing the TPM matrix must be non-negative and lie between 0 and 1. The addition of the entrance of each line must be equal to 1. The probabilities of the initial state of the system $P(0)$ may be represented by a line matrix.

$$P(0) = [P1\ (0),\ P2\ (0), \ldots, Pn\ (0)] \tag{3}$$

4. Methodology

4.1. Condition rating

The decision to employ Markov chains to predict service life, together with reliability theory, aims to consider uncertainties of degradation process until the structure reach the durability limit state. The condition rate may be classified based on the critical chloride concentration (C_{cr}) on the surface of the steel bar to define durability limit state.

4.2. Transition probability matrix

Markov process can be described through the following formula (Ross, 2000).

$$S_t = r(P)^t \tag{4}$$

S_t = State vector at time step t.
P = Transition probability matrix, P_{ij} represents the probability of process going from state i to state j.
r = Initial state vector.

The random variable vectors $x = [C_{cr}, C_o, x, D_c]$, where C_{cr} is the critical chloride concentration to initiate corrosion, C_o is the surface chloride concentration, x is the cover depth to reinforcement, and D_c is the diffusion coefficient of chloride ion, Fick's second law can be written in the simple form:

$$\frac{\partial c}{\partial t} = D_0 \frac{\partial^2}{\partial x^2} \tag{5}$$

in which D_0 is the constant coefficient of diffusion. The solution of the differential equation is presented above, for a semi-infinite domain with a uniform concentration at the structural surface, is given by:

$$C(x,t) = C_0\, erfc\,[x/(2\sqrt{D_0 t}] \tag{6}$$

where C_0 is the chloride concentration at the structural surface supposed constant in the time; *erfc* is the complementary error function. Here, Eq. (6) is used to evaluate the chloride concentration, $C(x, t)$, at a given depth and time into reinforced concrete structures.

The random variables C_{cr}, C_0, x, D_c can be generated by Monte Carlo Simulation and thus reliability index and probability of failure are calculated according to the following formulas.

$$\beta = \frac{\mu_{C_{cr}} - \mu_{C(x,t)}}{\sqrt{SD^2_{C_{cr}} + SD^2_{C(x,t)}}} \tag{7}$$

$$P_{(f)} = \varphi(-\beta) \tag{8}$$

φ = Standard normal distribution, β = Reliability index.

The probability of failure for a particular damage level will indicate the condition rating for a specific age of structure while the inspection is done. This probability of failure is used in transition probability matrix (TPM).

If five states of transition is considered, TPM matrix takes the following form:

$$P = \begin{bmatrix} p_{11} & p_{12} & 0 & 0 & 0 \\ 0 & p_{22} & p_{23} & 0 & 0 \\ 0 & 0 & p_{33} & p_{34} & 0 \\ 0 & 0 & 0 & p_{44} & p_{45} \\ 0 & 0 & 0 & 0 & 1 \end{bmatrix} \tag{9}$$

where P_{11}, P_{22}, P_{33}, P_{44} probability that the process will remain in the existing condition state. P_{12}, P_{23}, P_{34}, P_{45} probability that the process will pass into a higher condition state P_{55}=1 because the element cannot pass from condition state 5 to any other condition state.

Table 1. Condition rating of concrete.

Failure Extent	Condition Rating	Damage Level	Action Required
Safe	0	C_{cr} <0.2	No Maintenance
Fair	1	0.3 > C_{cr} ≥ 0.2	Repair
Poor	2	0.4 > C_{cr} ≥ 0.3	Repair
Critical	3	0.8 > C_{cr} ≥ 0.4	Repair
Failure	4	C_{cr} ≥ 0.8	Replacement

4.3. Repairing option

The maintenance policy can be described as "when the system hits state i, recovers it back to state j".

$$S_t = r(RP)^t \tag{10}$$

R=Repair matrix.

Repair action against deterioration of bridge can be represented by matrix form. However, the repair matrix is also a square matrix like TPM with same number of rows and columns as number of condition states are considered. In case of repair matrix, the elements above the diagonal are zero because repair action means the improvement of condition from deteriorating condition to good condition e.g. improvement from

$$3 \longrightarrow 1,\ 3 \longrightarrow 2,\ 2 \longrightarrow 1$$

So, in repair matrix, there will be elements corresponding to those state transition only and other value will be equal to zero. Three types of repair matrix are used for improvement of bridge deterioration which are shown below:

Repair Matrix 3:

	1	2	3	4	5
1	1	0	0	0	0
2	0	1	0	0	0
3	0	0	1	0	0
4	0	0	1	0	0
5	0	0	1	0	0

In this matrix, the value of elements 1-1, 2-2, 3-3 is 1 which means there will not be any change in this repair. Bridge element condition in state 4, 5 will be improved to state 3.

Repair Matrix 5:

	1	2	3	4	5
1	1	0	0	0	0
2	0	1	0	0	0
3	0	0.95	0.05	0	0
4	0	1	0	0	0
5	0	1	0	0	0

In this matrix, probability of elements 1-1 and 2-2 is 1 which means there will be no change in state. There is a probability that the 95% of bridge will be improved to state 2 from state 3 and all the bridges from states 4 and 5 will be improved to state 2. It is costlier than the previous repair matrix.

Repair Matrix 7:

	1	2	3	4	5
1	1	0	0	0	0
2	0.95	0.05	0	0	0
3	0.9	0.05	0.05	0	0
4	0	0	0	0	0
5	0	0	0	0	0

In this matrix, bridges in state 1 will remain in the same state as the probability is 1. 95% of bridges in state 2 will be improved to state 1. Bridges in state 3, there are 5% of bridges remain in the same state, 5% will be improved to state 2 and the remaining 90% will be improved to state 1. Bridges in state 4 and 5 will directly improve to state 1 as the probability is 1. It is costlier than the other two repair options**.**

If there is no maintenance, then system will deteriorate towards the "fail" state eventually. However, with appropriate maintenance interventions the system behaves periodically in the long run. Following is an example of maintenance policy (Fig. 1).

There are various state improvements of the structure in the above chart according to the consideration of different types of repairing. The structure has to be replaced when only it reaches to state 4 to come back to state 0 (Fig. 2).

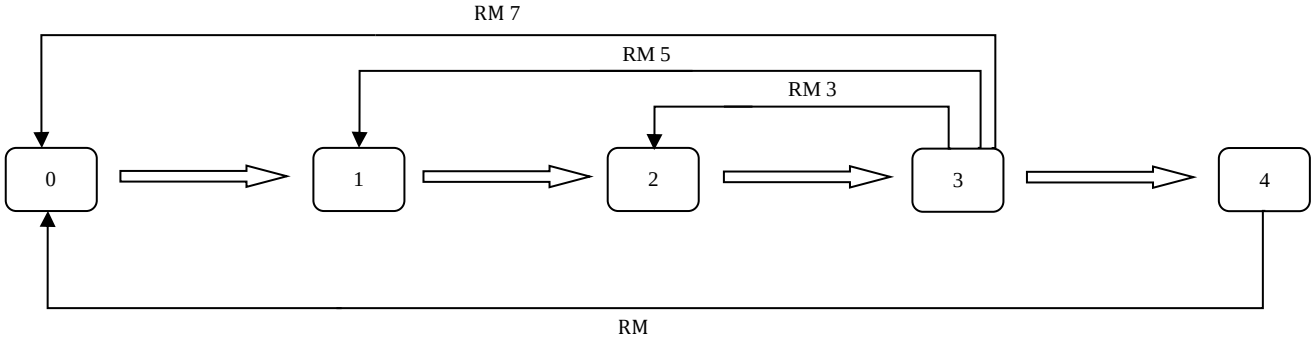

Fig. 1. Improvement capacity of RM 3, RM 5, RM 7 repair options.

5. Results and Discussions

In this paper, five types of concrete of different failure probabilities are used. The concrete of less failure probability is considered as stronger concrete. Repair options 3, 5, 7 are used to satisfy the dynamic expected condition.

Assuming, the costs for repair matrix 3, 5, 7 are 200 units, 500 units & 800 units respectively.

For C1 type concrete (0.98-0.02)

Here, 0.02 is the critical chloride concentration. The more the critical concentration, the less the stronger concrete.

Fig 3. shows bridge deterioration probability for C1 type concrete. It is stronger concrete and its remaining rate in its present state is 98%. Its rate going to next higher state is 2%. Fig. 3 shows that, C1 type concrete requires two of RM 3, one of RM 5 and one of RM 7 to satisfy the expected critical failure probability 0.3.

For C2 type concrete (0.90-0.10)

Here, 0.10 is the critical chloride concentration. As the value is small, so C2 type concrete is stronger concrete.

Fig. 4 shows bridge deterioration probability for C2 type concrete. It is stronger concrete and its remaining rate in its present state is 90%. Its rate going to next higher state is 10%. Fig. 4 shows that, C2 type concrete

requires three of RM 3, two of RM 5 and one of RM 7 to satisfy the expected critical failure probability 0.3.

For C3 type concrete (0.80-0.20)

Here, 0.20 is the critical chloride concentration. As the value is average, so C3 type concrete is average concrete.

Fig. 5 shows bridge deterioration probability for C3 type concrete. It is average concrete and its remaining rate in its present state is 80%. Its rate going to next higher state is 20%. Fig. 5 shows that, C3 type concrete requires four of RM 3, four of RM 5 and two of RM 7 to satisfy the expected critical failure probability 0.3.

For C4 type concrete (0.70-0.30)

Here, 0.30 is the critical chloride concentration. As the value is large, so C4 type concrete is weakest concrete.

Fig. 6 shows bridge deterioration probability for C4 type concrete. It is weaker concrete and its remaining rate in its present state is 70%. Its rate going to next higher state is 30%. Fig. 6 shows that, C4 type concrete requires nine of RM 3, four of RM 5 and two of RM 7 to satisfy the expected critical failure probability 0.3.

For C5 type concrete (0.60-0.40)

Here, 0.40 is the critical chloride concentration. As the value is largest, so C5 type concrete is weakest concrete.

Fig. 7 shows bridge deterioration probability for C5 type concrete. It is weakest concrete and its remaining rate in its present state is 60%. Its rate going to next higher state is 40%. Fig. 7 shows that, C5 type concrete requires nine of RM 3, six of RM 5 and four of RM 7 to satisfy the expected critical failure probability.

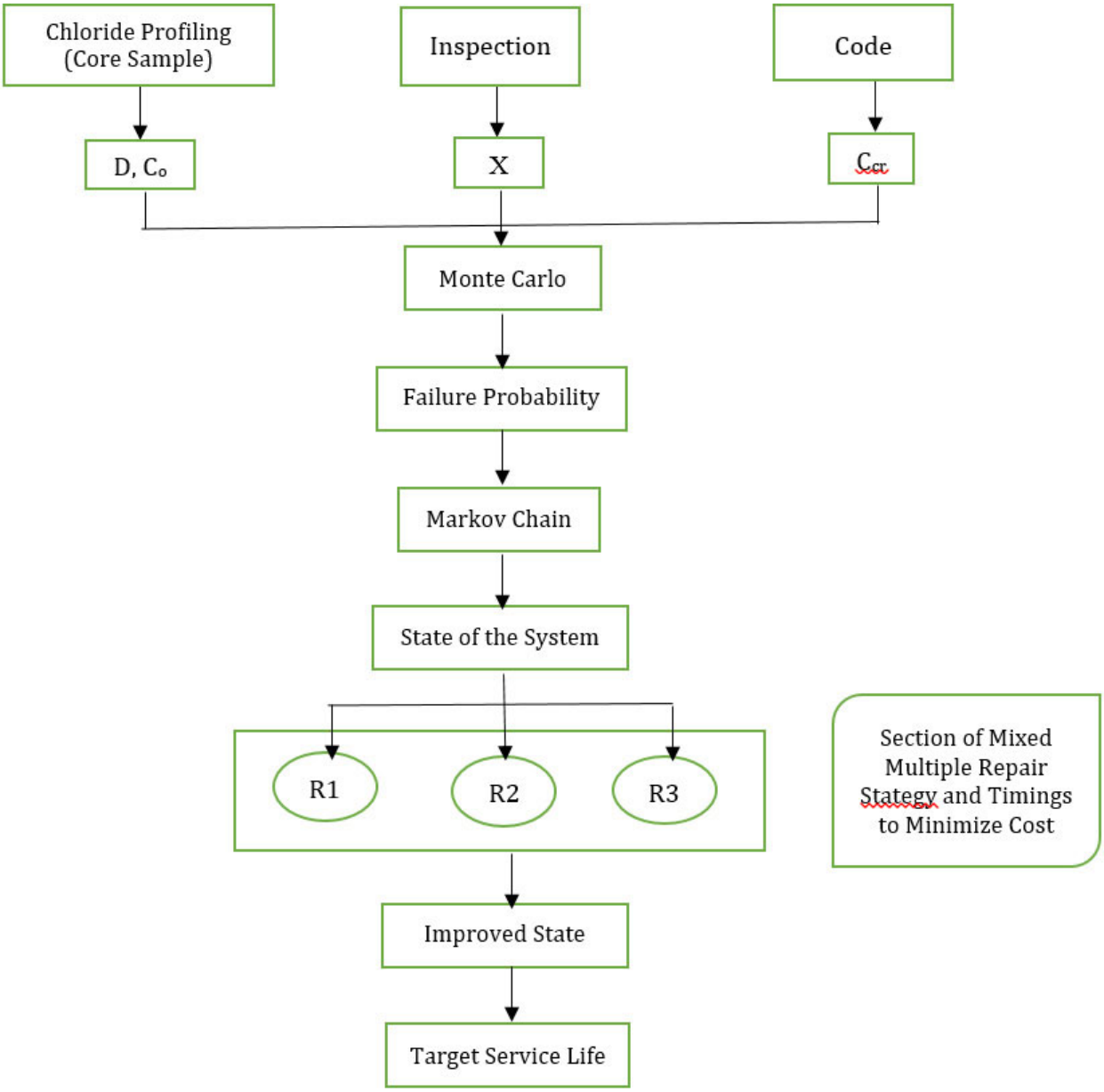

Fig. 2. Work flow of Simulation process of degradation of concrete.

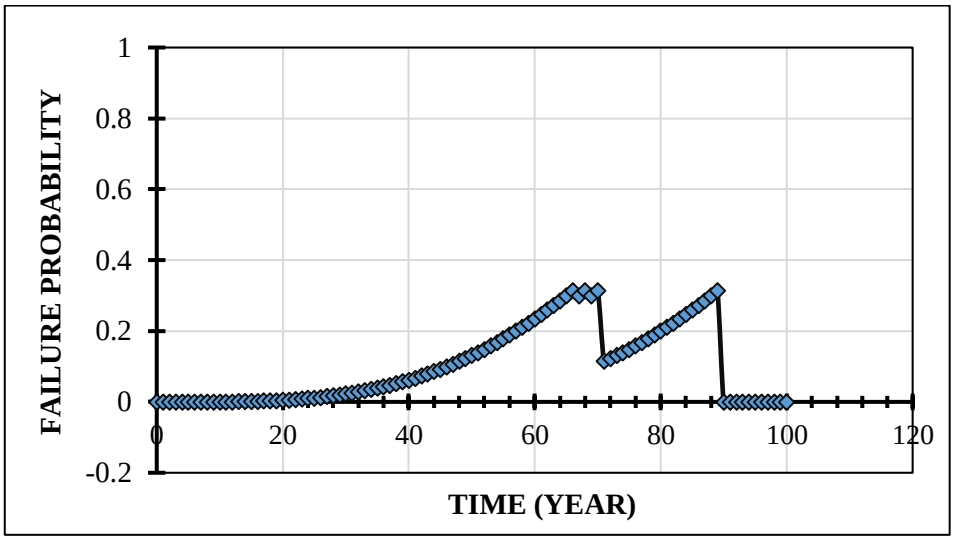

Fig. 3. Bridge deterioration probability for C1 type concrete.

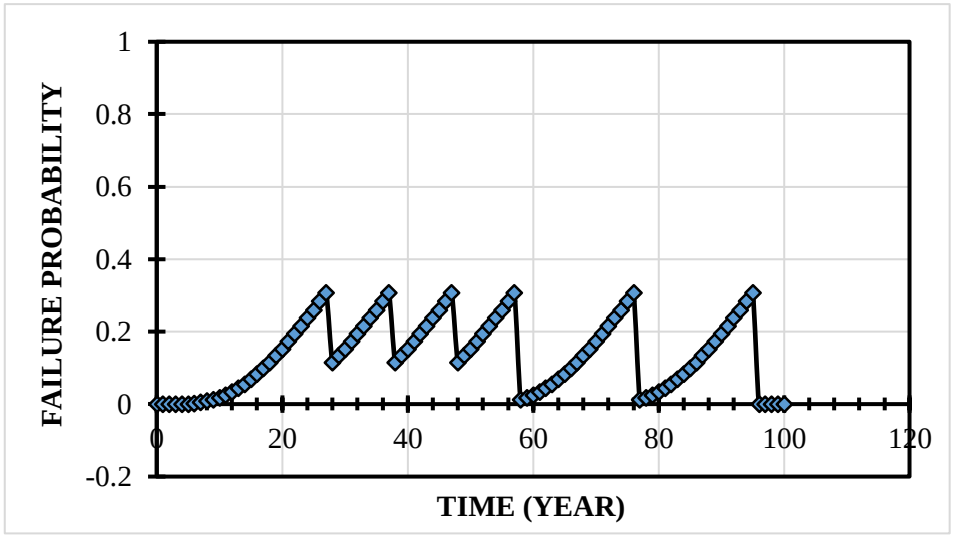

Fig. 4. Bridge deterioration probability for C2 type concrete.

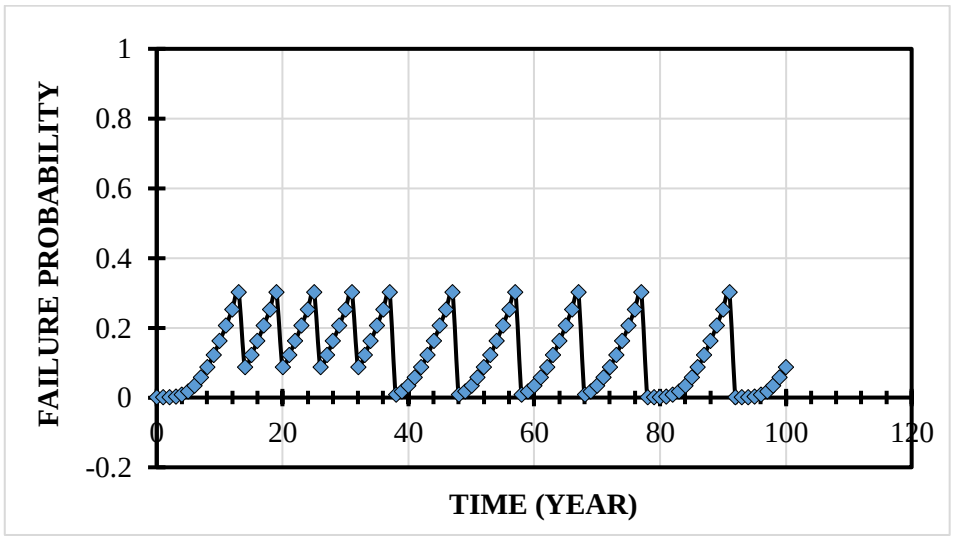

Fig. 5. Bridge deterioration probability for C3 type concrete.

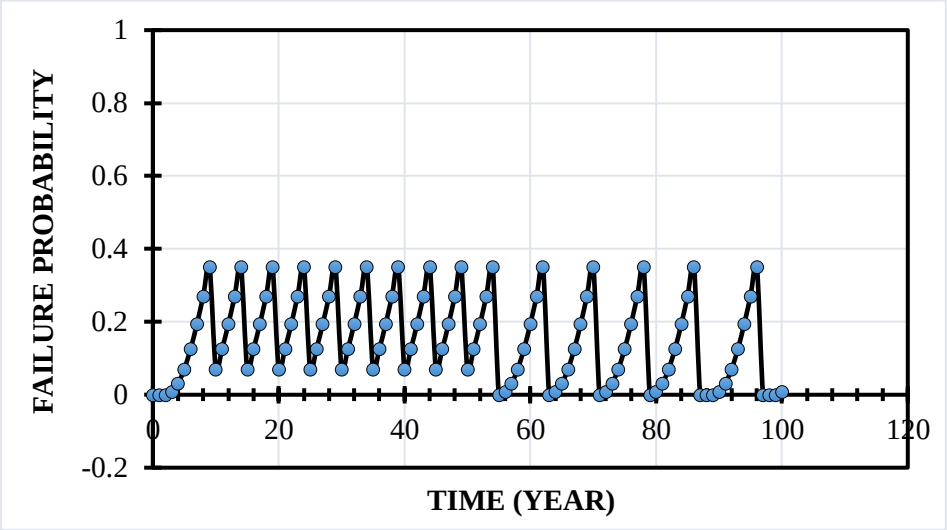

Fig. 6. Bridge deterioration probability for C4 type concrete.

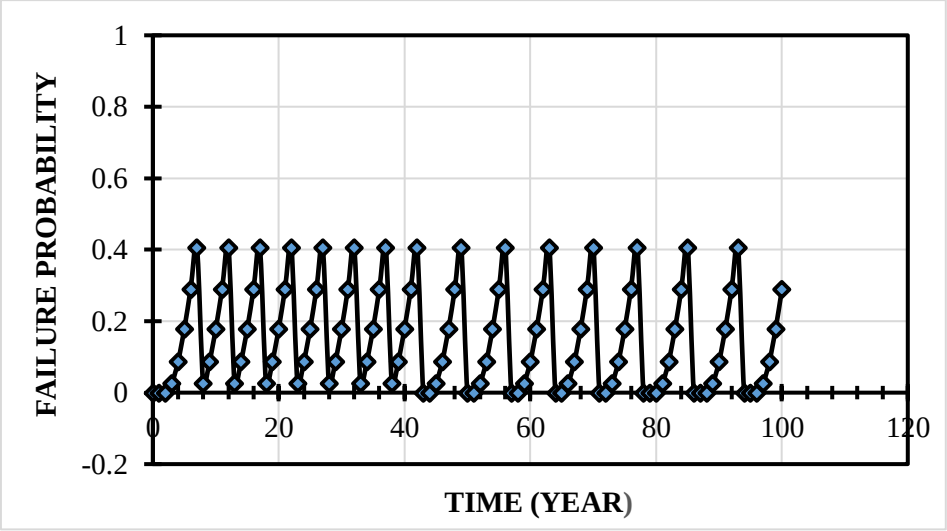

Fig. 7. Bridge deterioration probability for C5 type concrete.

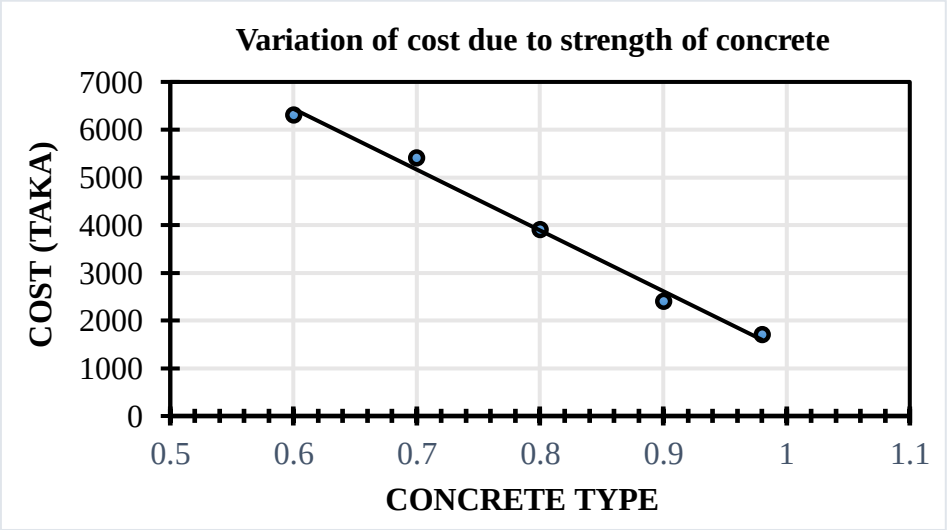

Fig. 8. Variation of life cycle cost according to strength of concrete.

6. Conclusions

The objective of this paper is to create multiple repair scenario from mix repair options and to optimize the life cycle cost. A deterministic prediction method will not be appropriate for deterioration modelling of bridge component. The Markov chain approach appears to offer a superior solution by using the percentage prediction method to develop the transition matrix. Using the developed transition matrices, some preliminary conclusions about deterioration of the bridge components can be made.

Fig. 8 shows variation of life cycle cost of five types of concrete (stronger to weaker) with specific critical failure probability with combination of mix repair. Here, we can see the life cycle cost for strongest concrete is less comparatively weakest concrete. As a result, weakest concrete will need a huge amount of cost applying repair options to satisfy the dynamic expected critical failure probability 0.3. Also for weakest concrete, large numbers of repair options are required and for stronger concrete, small numbers of repair options are required to satisfy the critical failure probability.

Acknowledgements

We want to express our gratitude to those who supported and helped a lot to complete the research. We would never have been able to finish our thesis without the guidelines of our research supervisor, Md. Shafiqul Islam, Professor, Department of Civil Engineering, Rajshahi University of Engineering & Technology (RUET), 6204 Rajshahi, Bangladesh. We would like to express our gratitude to our research supervisor for his constructive suggestion, persistent encouragement, valuable advice, inspiration, constant guidance, patience and commendable guidance through the time.

References

Elbehairy H (2007). Bridge Management System with Integrated Life Cycle Cost Optimization. *Ph.D thesis*, University of Waterloo, Waterloo, Ontario, Canada.

Hegazy T, Elbeltagi E, El-Behairy H (2007). Bridge Deck Management System with integrated life cycle cost optimization. Transportation Research Record: *Journal of the Transportation Research Board*, 1866(1), 44-50.

Hrvatske R (2013). Bridge condition forecasting for maintenance optimization. *Journal of the Croatian Association of Civil Engineers*, 65(12), 1079-1088.

Li L, Sun L, Ning G (2014). Deterioration prediction of urban bridges on network level using Markov chain model. *Mathematical Problems in Engineering*, 2014, 728107.

Nogueira CG, Leonel ED, Coda HB (2012). Probabilistic failure modelling of reinforced concrete structures subjected to chloride penetration. *Journal of Advanced Structural Engineering*, 4(1), 1-14.

Possan E, Andrade J (2014). Markov Chain and reliability analysis for reinforced concrete structure service life. *Materials Research*, *17(3),* 593-602.

Saeed Hasan Md, Setunge S, Law DW, Koay Y (2014). Forcasting deterioration of bridge components from visual inspection data. *International Journal of Engineering and Technology*, 7(1), 40-44.

Setunge S, Saeed Hasan Md (2011). Concrete bridge deterioration prediction using Markov-chain model. *Digital Library*, 17(3), 593-602.

Shafiqul Islam Md, Kanti Baul P, Haque O (2018). Observation of chloride permeability between normal aggregates concrete and recycled aggregates concrete containing fly ash and clay. *Challenge Journal of Concrete Research Letters,* 9(4), 103-109.

Challenge Journal of Concrete Research Letters

Research Article

Effect of w/c ratio and cement content on diffusivity of chloride ion in concrete: A molecular dynamics study

Rokonuzzaman Rokon [a], Md. Shafiqul Islam [a,*], Nusrat E. Mursalin [b]

[a] *Department of Civil Engineering, Rajshahi University of Engineering & Technology, Kazla 6204, Rajshahi, Bangladesh*
[b] *Department of Civil Engineering, Bangladesh Army University of Engineering & Technology, Qadirabad Cantonment, Natore, Bangladesh*

ABSTRACT

When a reinforced structure is exposed to marine environments, chloride-induced corrosion occurs and it decreases the durability and performance of the structure. The degree of humidity, the presence of cracks, environmental conditions, w/c ratio, and cement content are the influencing factors for chloride ion ingress into concrete. All of them, w/c ratio and cement content are treated as the most crucial factors on diffusion. This paper focus on Molecular Dynamics (MD) simulation method to determine the diffusion coefficient of chloride ion in concrete. The effect of w/c ratio and cement content on the diffusivity of chloride ion is also evaluated. The diffusion coefficients are obtained $2.88x10^{-12}$ m^2/s, $3.13x10^{-12}$ m^2/s, and $3.61x10^{-12}$ m^2/s respectively for different w/c ratio of 0.40, 0.45 and 0.50 with constant cement content. Again the diffusion coefficient are calculated $4.6x10^{-12}$ m^2/s, $3.13x10^{-12}$ m^2/s, $2.78x10^{-12}$ m^2/s respectively for different cement content of 300 kg/m^3, 350 kg/m^3 and 400 kg/m^3 with constant w/c ratio. The simulation results clearly indicate that the diffusion coefficient of chlorine was affected by w/c ratio and cement content significantly.

ARTICLE INFO

Article history:
Received 1 July 2019
Revised 19 November 2019
Accepted 16 December 2019

Keywords:
Concrete
Chloride
Water-cement ratio
Cement content
Diffusion coefficient
Molecular Dynamics

1. Introduction

Chloride penetration into concrete is of great importance on the durability of reinforced concrete. When a reinforced concrete structure is exposed to marine environments, chloride-induced corrosion takes place and reduces the susceptibility of reinforcement. If a threshold value of chloride content is accumulated with the presence of oxygen or moisture content, the corrosion of reinforcement will initiate (Al-Gadhib, 2010).

A high alkaline environment, which is formed by hydration products of cement, creates a passivated film on the embedded steel surface. So the surface remains chemically stable to protect the steel from corrosion. When a certain amount of chloride content penetrates, it destroys the alkaline environment and disrupts the passivated film (Townsend et al., 1981) and steel surface becomes vulnerable to initiate corrosion.

There are several mechanisms to ingress chlorine through concrete. In all of the mechanisms, it is assumed that diffusion is the most basic phenomenon of chloride ion penetration (Erdoğdu et al., 2004). This diffusion is controlled by some external and internal parameters like the thickness of cover, pore structure, w/c ratio and cement content etc. (Al-Gadhib, 2010). Again initiation of corrosion time is very much dependent on the diffusivity property of concrete.

The service life of a reinforced concrete structure can be reliably predicted by diffusivity of concrete. So the determination of diffusion coefficient of chloride ion is very essential to analyze chloride-induced corrosion initiation time as well as predict the service life of a concrete structure in a marine environment, deicing salts, and coastal areas.

* *Corresponding author*. E-mail address: rokonruet002@gmail.com (R. Rokon)
ISSN: 2548-0928 / DOI: https://doi.org/10.20528/cjcrl.2019.04.002

2. Theory

2.1. Chloride penetration

The concentration of chloride at the surface of embedded steel in concrete as well as chloride ion transport can be modeled by Fick's second law of diffusion. It is frequently used in the following form for one-dimension:

$$\frac{\partial C}{\partial t} = D\frac{\partial^2 C}{\partial x^2} \tag{1}$$

Where C is the total chloride content, t is time and D is the diffusion coefficient. The following boundary conditions are considered:

- a single spatial dimension x, ranging from 0 to 1 for the semi-infinite case,
- $C = C_o$ at $x = 0$ and $t > 0$ (boundary condition),
- $C = 0$ at $x > 0$ and $t = 0$ (initial condition).

where, C_o is the initial chloride content, x is the distance from edge of the concrete.

An analytical solution of Eq. (1) has the form:

$$C_x = C_s\left[1 - erf\left(\frac{x}{2\sqrt{Dt}}\right)\right] \tag{2}$$

where, C_x is the chloride ion concentration at depth x after exposure time t for a surface chloride concentration of C_s at the concrete surface and the expression *erf* is the Gaussian error function.

The behavior of concentration of chloride ion in concrete structures is adequately described by Eq. (1) and its analytical solution.

2.2. Lennar-Jones pair potential

Any two molecules at a long separation distance attract each other and when come closer repel each other (Hirschfelder et al, 1964). The intermolecular force between chloride ions i and j separated a distance r_{ij} is expressed by Lennard-Jones pair potential as the following equation:

$$U_{ij} = 4\varepsilon\left[\left(\frac{\sigma}{r_{ij}}\right)^{12} - \left(\frac{\sigma}{r_{ij}}\right)^{6}\right] \tag{3}$$

where r_{ij} is the intermolecular distance, U_{ij} is the potential energy, ε is the depth of the LJ potential well, σ is the collision diameter.

In computer simulation, the potential must be truncated at a point named cutoff radius, $R_{cut.}$ If the separation between two molecules becomes greater than the cutoff radius, the intermolecular forces between the molecules will be zero. Actually, the forces exerted between two molecules at a large distance are very small and it can be neglected (Rapaport, 2004) which helps to reduce the computational effort.

$$U_{ij} = \begin{cases} U_{ij} \neq 0, & r_{ij} \leq R_{cut} \\ 0, & r_{ij} > R_{cut} \end{cases} \tag{4}$$

2.3. Theory of molecular dynamics

Molecular Dynamics (MD) is a computer simulation process in which physical movements of particles or atoms are studied. In this method, particles are allowed to interact for a certain period of time, giving a view of the motion of particles (Al-matar et al., 2012)

Molecular dynamics, in its usual form applies numerical integration for Newton's equation of motion (Nissen, 2016).

$$F_i = m\frac{d^2 r}{dt^2} \tag{5}$$

where, F_i is net force on the i-th particle, m is mass and r is the position vector of the i-th particle.

By integrating Newton's equation of motion, new positions and velocities are obtained after time step Δt. One of the most used algorithms is the velocity Verlet algorithm which is used for computing the new positions of molecules.

$$r(t + \Delta t) = 2r(t) - r(t - \Delta t) + \frac{F(t)}{2m}\Delta t^2 \tag{6}$$

where Δt is the time steps in MD simulation.

3. Literature Review

An enormous experimental and numerical study has been seen previously in the determination of the diffusivity of chloride ion through concrete structures based on different parameters and methods. Al-Gadhib (2010) studied the influence of w/c ratio and binder content on chloride ingress in concrete and established a numerical model based on finite element method to predict the diffusion of chloride ion into concrete. Erdoğdu et al. (2004) determined the apparent diffusion coefficient of chloride ion using open-circuit potential measurements and showed the time required to initiate corrosion comparison between synthetic seawater and NaCl solutions exposure.

Wang et al. (2005) proposed a mathematical model for the simulation of electrochemical chloride removal (ECR) process to predict the ionic mass transport associated with chloride ingress into concrete or hydrated cement paste from a saline environment. Li et al. (2015) presented a new transport model to describe the penetration of chlorides in cement-based materials with the concept of double porosity to reflect the influence of pore size distribution on the transport of ionic species in porous materials. Nissen (2016) analyzed the sensitivity of the input parameters in the fib model for chloride ingress and validation of the model for short exposure times. the influences of the meso-structural parameters, including aggregate distribution, aggregate shape, diffu-

sivity properties of the ITZ, water/cement ratio and aggregate content. Du et al. (2014) studied using FEM on the diffusivity of chloride into concrete. Also corrosion rate depends on different w/c ratio presented by Wachira (2019).

In the present study, the transportation of chloride ion into concrete under the atmospheric chloride environment is investigated. Molecular Dynamics method, a widely used plausible simulation method for time dependent response, is carried out to simulate the ingress process. Diffusion coefficient of chlorine ion into concrete is determined to elucidate the chloride transport mechanism. Effects of water-to-cement ratio and cement content on the chloride transport and microstructure are evaluated.

4. Methodology

4.1. Mix proportion

In our simulation, different types of specimen are used which is shown in Table 1. The specimen is considered as crack free and the cement type is Ordinary Portland Cement (OPC).

Table 1. Mix proportion of specimen.

	Simulation ID	w/c ratio	Cement content (kg/m³)
MD simulation with constant cement content	MD1	0.40	350
	MD2	0.45	
	MD3	0.50	
MD simulation with constant w/c ratio	MD4	0.45	300
	MD2		350
	MD5		400

4.2. Simulation geometry

In our MD simulation, we considered a 2D simulation cell with a defined grid size. All parameters of the simulation cell are shown in Table 2. We calculated the total node in our cell 100 which is actually the total number of particles in our simulation. Chloride environment is subjected from one side. The number of chloride ion and oxygen ion are calculated using defined w/c ratio, cement content and which is shown in Table 3.

Table 2. Details of parameters in the MD simulation.

Property	Dimensions
Cell dimensions, μm	15 x 15
Grid size, μm	1.5
No of particles	100
Temperature, K	298
Cutoff radius, μm	3

Table 3. Total number of particles.

Simulation ID	No of Chlorine ion	No of Oxygen ion
MD1	5	95
MD2	6	94
MD3	7	93
MD4	8	92
MD5	6	94
MD6	4	96

4.3. Simulation setting

In this work, the NVE (microcanonical) ensemble was used in a molecular dynamics simulation to equilibrate the total system energy. The time step size was 0.001 s and the total number of simulation cycle was 100. So the total simulation time was 0.1 s. After every 0.01s, all the positions of the particles were saved for further calculations.

At the first of the simulation, we arranged the chloride and oxygen particles in our cell. Initial velocities were generated from Boltzmann's distribution and shifted all velocities that momentum is zero. To adjust kinetic energy to the desired value, we rescaled the resulting velocities. The periodic boundary condition was applied along the *x* and *y* dimensions.

The interactions between Cl-Cl, Cl-O, and O-O were considered and Lennard-Jones pair potential was used to determine the intermolecular forces using Eq. (3). The interaction between the walls and particles was eliminated. Velocity Verlet algorithm was used to integrate Newton's equation of motion using Eq. (6).

After completing the simulation, Mean Square Displacement (MSD) was calculated using the following equation.

$$MSD = \frac{1}{N}\sum_{i=1}^{N}(r(t) - r(t=0))^2 \quad (7)$$

where, N is the total number of particles, $r(t)$ is the position of particles after time t, $r(t = 0)$ is the initial position of the particles.

For further analysis, we plotted the MSD vs time curve in Microsoft EXCEL and the slope of the curve was also determined which is the diffusion coefficient of chloride ion. All MD simulation code was written in FORTRAN 95.

5. Results and Discussion

5.1. Effect of w/c ratio on chloride diffusion

Fig. 1 illustrates the total energy profile of the molecular dynamics simulation at a temperature of 298 K. The total energy is the sum of kinetic energy and potential energy at a certain temperature. From Fig. 1, we can say that total energy and kinetic energy remain steady but potential energy is fluctuating within the simulation. The kinetic energy is positive within a range of 2600 J/mol to 2844 J/mol approximately. The potential energy is both negative and positive within a range of -55 J/mol to 190 J/mol approximately. Therefore, the total energy is the sum of kinetic and potential which comes out to be nearly 2790 J/mol.So, the conservation of total energy verifies that our MD simulation is scientifically plausible and we can use it to calculate the diffusion coefficient of chloride ion.

The Mean Square Displacement (MSD) after every time steps is shown in Table 4 for all MD simulation.

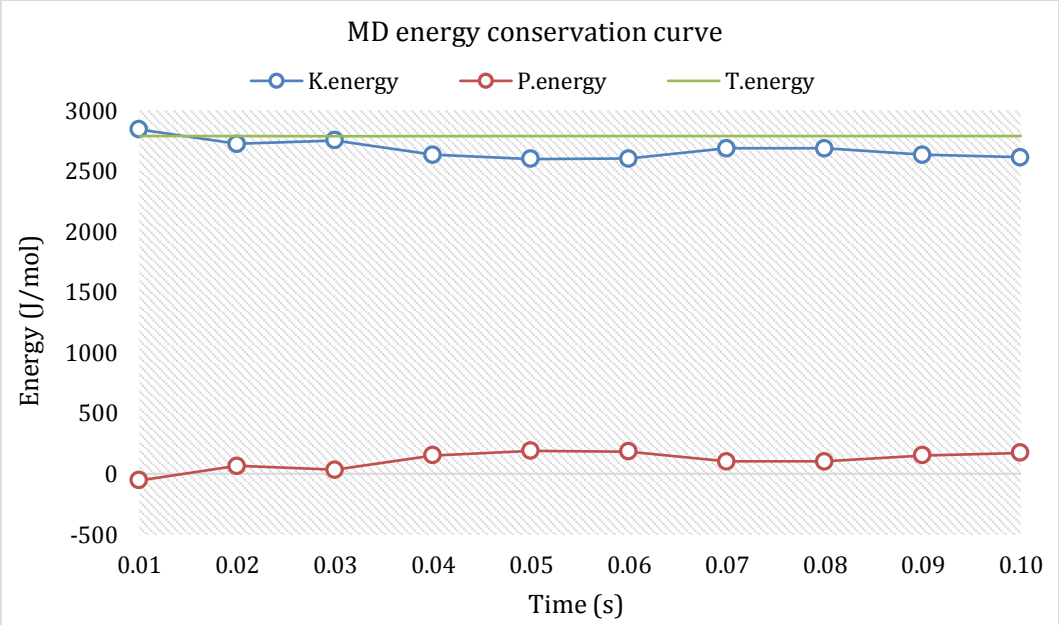

Fig. 1. Total energy conservation within total simulation time.

Table 4. Mean Square Displacement (MSD) with varying time steps.

	MD simulation ID				
Time (s)	MD1 Δr^2 x E-12 (m^2)	MD2 Δr^2 x E-12 (m^2)	MD3 Δr^2 x E-12 (m^2)	MD4 Δr^2 x E-12 (m^2)	MD5 Δr^2 x E-12 (m^2)
.01	0.0042109	0.00421090	0.003699	0.00388257	0.00579376
.02	0.01620982	0.01620982	0.013888	0.01481927	0.02249039
.03	0.03455199	0.03455199	0.027284	0.03158704	0.04766204
.04	0.05942794	0.05942794	0.046844	0.05863773	0.07779074
.05	0.08939900	0.08939900	0.077533	0.09783581	0.11081360
.06	0.12073558	0.12073558	0.117699	0.14484510	0.14225333
.07	0.15468196	0.15468196	0.164876	0.19455749	0.16952453
.08	0.19222454	0.19222454	0.214346	0.25516860	0.19513153
.09	0.23538684	0.23538684	0.26537	0.33342304	0.22046513
.10	0.28534462	0.28534462	0.323554	0.42646436	0.24593148

MSD versus time curves for all simulations are shown in Fig. 2. To calculate the diffusion coefficient of chloride ion accurately, linear regression was used to fit the MSD curve. The slops of the curves which are desired diffusion coefficient are $2.88x10^{-12}$ m^2/s, $3.13x10^{-12}$ m^2/s and $3.61x10^{-12}$ m^2/s for MD1, MD2 and MD3 respectively. It is clearly seen that, as expected, with the increasing of w/c ratio, the higher is the diffusivity of chlorine which is presented in Fig. 3 and thus the chloride movement is faster.

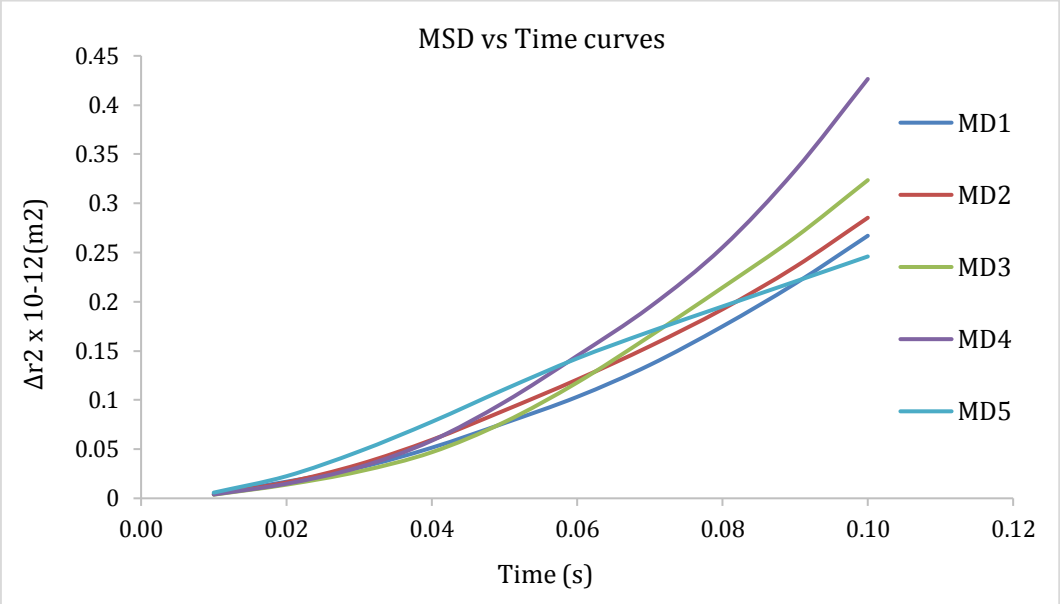

Fig. 2. MSD vs time curve to obtain diffusion coefficient of chloride ion.

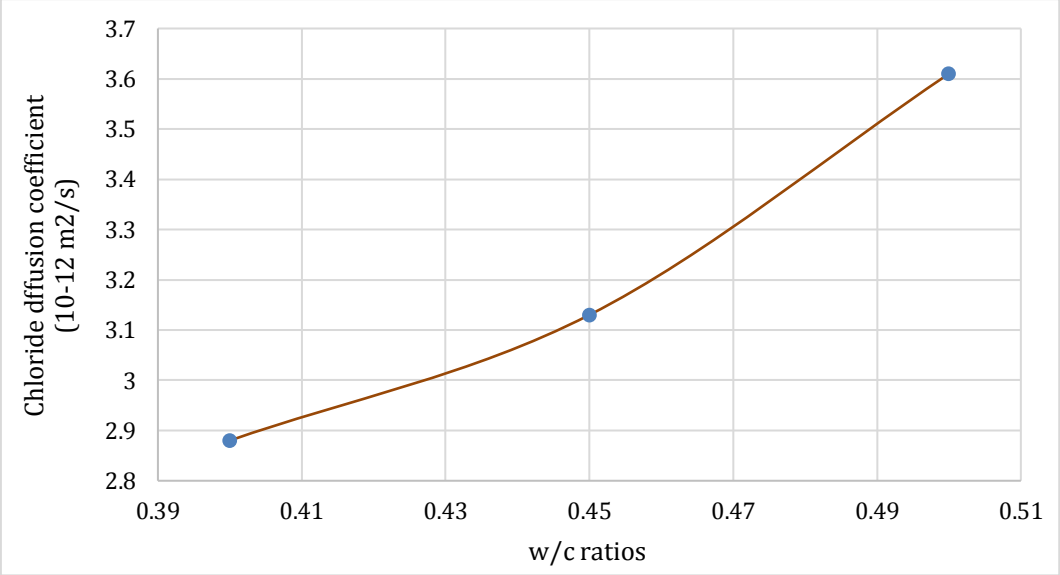

Fig. 3. Chloride diffusion coefficient with different w/c ratios.

5.2. Effect of cement content on chloride diffusion

From MSD versus time curve in Fig. 2, we obtained diffusion coefficient of chloride ion for MD4, MD2, and MD5 are $4.6x10^{-12}$ m^2/s, $3.13x10^{-12}$ m^2/s and $2.78x10^{-12}$ m^2/s, respectively. As expected, the higher the cement content, the diffusion coefficient is lower which is shown in Fig. 4 and thus chloride requires a longer time to reach the same level as that for the lower cement content.

It is clearly seen that the diffusion coefficient of chlorine ion may change significantly with changing of w/c ratio and cement content. With increasing the w/c ratio, chloride diffusivity is also increased. A similar trend is seen for varying cement content in which the lower the cement content, the higher the diffusivity which is more plausible from simulation results.

6. Conclusions

This paper deals with MD simulation to determine the diffusion coefficient of chlorine ion. Again the effect of w/c ratio and cement content on the diffusion coefficient of chloride ion into concrete also evaluated. Then the following conclusions are made:

- With a varying w/c ratio 0.40, 0.45 and 0.50 at a constant cement content, it is evaluated that the diffusion coefficient of chloride ion is increased linearly almost 110% respectively.
- At a constant w/c ratio and cement content varies with 300 kg/m^3 to 350 kg/m^3, the diffusion coefficient of chloride ion is decreased linearly almost 150%. Again cement content varies with 350kg/m^3 to 400 kg/m^3, it is decreased almost 112% .

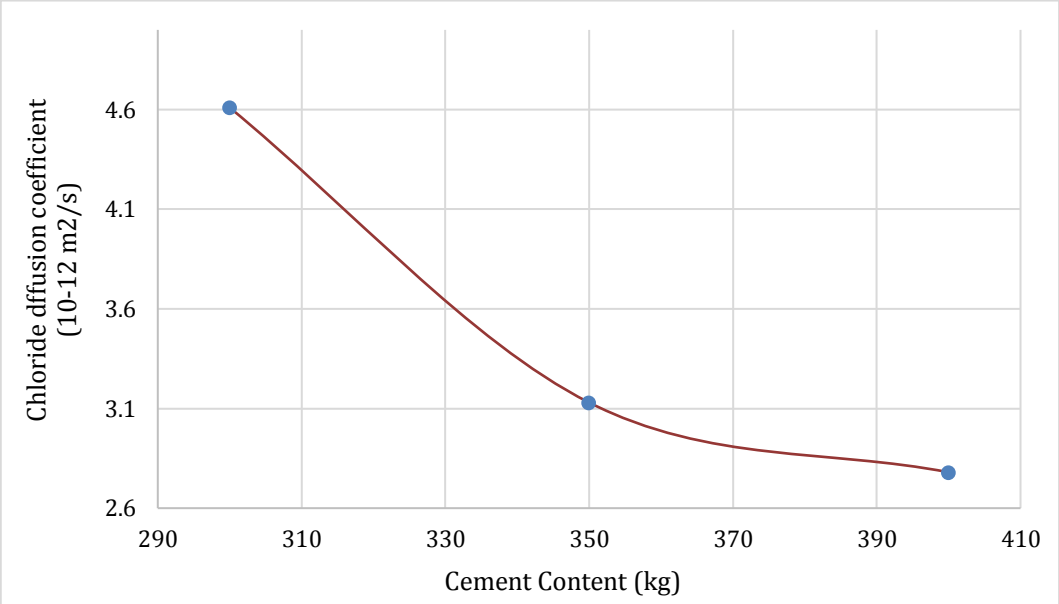

Fig. 4. Chloride diffusion coefficient with different cement content.

Acknowledgements

This work was done as a final year thesis when the corresponding author was studying for his BSc Degree, Course No. CE 4000 & Course Title: Project & Thesis at Rajshahi University of Engineering & Technology.

References

Al-Gadhib AH (2010). Numerical simulation of chloride diffusion in RC structures and the implications of chloride binding capacities and concrete mix. *International Journal of Civil & Environmental Engineering,* 10(5), 19-28.

Al-matar A, Tobgy AH, Al-Faiad MA (2012). Self diffusion coefficient of Lennard-Jones fluid using temperature dependent interaction parameters at different pressures. *Sixth Jordan International Chemical Engineering Conference*, Amman, Jordan.

Erdoğdu Ş, Kondratova IL, Bremner TW (2004). Determination of chloride diffusion coefficient of concrete using open-circuit potential measurements. *Cement and Concrete Research,* 34, 603-609.

Hirschfelder JO, Curtiss CF, Bird RB (1964). Molecular Theory of Gases and Liquids. John Wiley and Sons, New York.

Li LY, Easterbrook D, Xia J, Jin WL (2015). Numerical simulation of chloride penetration in concrete in rapid chloride migration. *Cement and Concrete Composites,* 63, 113-121.

Nissen T (2016). Chloride Ingress in Concrete. *Ph.D thesis*, Norwegian University of Science and Technology, Gjøvik, Norway.

Rapaport DC (2004). The Art of Molecular Dynamics Simulation, (2nd edition). Cambridge University Press, New York.

Townsend HE, Cleary HJ, Allegra L (1981). Breakdown of oxide films in steel exposure to chloride solutions. *NACE Corrosion,* 37, 384-391.

Wachira JM (2019). Effects of chlorides on corrosion of simulated reinforced blended cement mortars. *International Journal of Corrosion*, 2019, Article ID 2123547.

Wang Y, Li LY, Page CL (2005). Modelling of chloride ingress into concrete from a saline environment. *Building and Environment,* 40(12), 1573-1582.

Xiuli Du, Liu Jin, Guowei Ma (2014). A meso-scale numerical method for the simulation of chloride diffusivity in concrete. *Finite Elements in Analysis and Design*, 85, 87-100.

Challenge Journal of Concrete Research Letters

Research Article

Behavior improvement of self-compacting concrete in hot weather

Mounir M. Kamal, Zeinab A. Etman *, Alaa A. Bashandy, Mohammed Nagy

Department of Civil Engineering, Menoufia University, Shebin ElKoum, Menofia, Egypt

ABSTRACT

The main aim of this research is studying the effect of hot weather on the properties of self-compacting concrete and conventional concrete in both fresh and hardened state. Also, this research extends to improve the behavior of self-compacting concrete in hot weather. The main parameters were surrounding weather temperature (5°C, 20°C and 35°C), concrete materials temperatures' (25°C, 50°C), curing temperatures (25°C and 50°C) and admixtures (using a retarder). Two stages were carried out to achieve the research aim. The behavior of self-compacting concrete compared to conventional concrete was evaluated in the first stage. Based on the first stage, attempts to enhance the concrete properties were evaluated in the second stage. Precautions on mixing and placing concrete in these climates are considered. Results are a drive in terms of; workability tests, compressive strength, splitting tensile strength, and flexural strength. Test results showed that self-compacting concrete behavior and strengths were better than conventional concrete. Slump test, J-ring and V-funnel test were used to evaluate the fresh properties of the self-compacting concrete. Drying shrinkage of self-compacting concrete in hot weather were also evaluated.

ARTICLE INFO

Article history:
Received 9 November 2019
Revised 7 December 2019
Accepted 16 December 2019

Keywords:
Hot weather
Concrete
Self-compacting
Conventional
Improving
Retarder

1. Introduction

Hot weather is the major reason of plastic shrinkage and cracks. Those cracks enhance bad chemicals as O_2, CL-, SO_4(-2) and CO_2 inside the concrete mix so that those cracks are determined the main reason of undesired strength results of concrete structures in hot weather (Nasir et al., 2016). Factors such as high temperature of the surrounding air, low relative humidity, the increase in wind speed and the continuous direct solar radiation affects badly on concrete at its fresh stage and during hardening processes (Al-Amoudi et al., 2007). Plastic shrinkage, cracks and strength reduction are results to exposing the structure to hot weather which led to the increase of concrete mix temperature and evaporation rate with a reduction in the structural safety (Ahmadi, 2000). Attempting to deal with such hard conditions, some important precautions must be taken. Self-compacting concrete is a concrete that flows under its own weight through restricted sections without segregation or bleeding. It's one of the highly workable types of concrete which also has high performance and suitable strength (EFNARC, 2005). Cooling concrete materials before use, the early concrete curing, and using suitable curing methods after concrete cast help overcoming such hard conditions. The results carried out by Al-Feel and Al-Saffar (2009) showed that Self-compacting concrete gives high early compressive strengths when taking previous precautions.

The nature of SCC is the increasing ratio of fine aggregates (F.A) to coarse ones (C.A) when comparing it to the conventional concrete as the ratio is (F.A/C.A = 1.22) so that, many practical applications have been discussed in researches to make sure that mechanical and durability properties are the same like conventional normally vibrated concrete especially in the hardened case. In hot weather conditions, the recommendations are clearly stated in the ACI 2010 (Mouret et al., 2003). The study of Park et al. (2017) showed that water contents, hydration products and the pore structures are the main affecting factors on strengths. The work was carried out under typical summer conditions, but the elevated hot temperatures didn't affect the early age strengths of concrete. On the long term, there was a strength loss because of the reduction of hydration and the porosity increase (EFNARC, 2005).

* *Corresponding author*. Tel.: +2-01-009-727355 ; E-mail address: :zeinab.etman@sh-eng.menofia.edu.eg (Z. A. Etman)
ISSN: 2548-0928 / DOI: https://doi.org/10.20528/cjcrl.2019.04.003

2. Experimental Program

The innovation in this research is the comparative study of the properties and the behavior of the self-compacting concrete compared to conventional concrete at hot weather. Also, how to improve its performance under hot weather. The importance of this research is to provide sufficient data for the researchers and engineers that concerns in using self-compacting concrete in the desert sites or such places with hot weather. 13 mixes for each type of concrete were casted.

2.1. Materials

The type of used cement is the ordinary Portland cement CEM I 52.5 N from the Suez factory. The Egyptian Standard Specification (E.S.S. 4756-1, 2012) is satisfied. The fine aggregate is the natural siliceous sand which satisfies the (E.S.S 1109, 2008). The mechanical properties of fine aggregates are shown on Table 1. The coarse aggregate is natural crushed dolomite with a maximum size of 10 mm satisfying ASTM C33 (2018), the particles were angular and irregular. According to the Egyptian code of practice, clean drinking fresh water was used for mixing and curing procedures. A high range water reducer for self-compacting concrete as a third generation superplasticizer, is used as concrete additive that facilitates extreme water reduction, excellent flowability at the same time optimal cohesion and highest self-compacting behavior. It meets the requirements of ASTM C494 Types G and F and BS EN 934 (2012). A highly effective super plasticizer with a set retarding effect for producing free-flowing concrete in hot climates is used that complies with ASTM C494 (2017) Types G and F and BS 5075 (2012) part 3. Fly ash is also used for producing a proper self-compacting mix according to the (E.C.P. 203, 2017). The method used for the concrete mix design was the CBI. The concrete mixture is designed to give at 28-day a compressive strength of 400 kg/m^2. The suitable mix design has the following constituents as shown in Table 2.

Table 1. Physical and mechanical properties of sand used.

Description	Value
Volume weight (t/m^3)	1.73
Specific gravity	2.6
Absorption (%)	0.78
Voids ratio (%)	33.81
Fineness modulus	2.61

Table 2. Mix proportions.

Code	Water (kN/mm^3)	Cement (kN/mm^3)	Sand (kN/mm^3)	Dolomite (kN/mm^3)	F.A. (%)	S.P. (%)	R2004 (%)
NC	1.8	4.5	6	11.617	----	----	----
SCC	1.53	4.5	9.9	8.2	2	2	----
HNC	1.53	4.5	6.15	11.94	----	----	2
HSCC	1.53	4.5	9.78	8.1	2	2	2

NC: Normal concrete, SCC: Self-compacting concrete, HNC: Hot weather normal concrete,
HSCC: Hot weather self-compacting concrete,
F.A.: Fly ash; an additive for producing the self-compacting concrete,
S.P.: A high range water reducer for self-compacting concrete,
R2004: A highly effective super plasticizer with a set retarding effect

Fig. 1. Crushed ice used for cooling mixing water.

Fig. 2. Heating mixing materials in the oven.

Each material is weighted accrual for the required accuracy. The surface moisture and the effective absorption of aggregate especially sand greatly affect the amount of mixing water. It's very important to determine the properties of aggregate to keep the amount of water content. In order to obtain a uniform concrete mix, mixing was performed using a mixer with high efficiency by feeding the materials in the proper order. The materials were mixed for a proper periods for 2 minutes of normal weather mixes and heated in the laboratory oven for about 30 mins reaching more than 50°C for hot weather mixes.

Charging sequence is coarse aggregate, fine aggregate, and the cement. After 2 minutes from starting time, water of different temperatures (5°C, 20°C and 35°C) with any superplasticizer is added to the mix gradually the mixer is still rotate after adding water with the superplasticizer for 3 minutes to insure the full mixing of the concrete components. Water at 5°C were reached by using crushed ice and at 35°C were reached by using boiling water leaving it in the laboratory normal weather for about 10 mins as shown in Figs. 1 and 2.

The concrete was charged out from the mixer; the slump, j-ring and v-funnel tests were performed to evaluate the fresh properties of the self-compacting concrete according to Egyptian Standard Specifications (E.S.S.). The concrete was placed in the molds. All specimens of both normal and self-compacted concrete were kept at molds for 24 hours. After 24 hours they were removed from the molds and immerged in clean water of temperature of 25°C for curing at 25°C. Other specimens were immerged in clean water of 50°C temperature using a heater for curing at 50°C until taken out for tested.

2.2. Testing of hardened concrete

Three tests were conducted to obtain hardened concrete properties as follow:

1. Compressive strength test using 78 concrete cubes of 100*100*100 mm length for each type of concrete.
2. Splitting tensile strength test using 52 concrete cylinders of 200 mm length and 100 mm diameter for each type of concrete.
3. Flexural strength test using 26 concrete prisms of 500 mm length and a cross-section of 100 mm for each type of concrete.
4. Dry shrinkage test using 26 concrete prisms of 250 mm length and a cross-section of 70 mm for each type of concrete as shown in Table 3.

3. Results and Discussion

3.1. Fresh properties

As shown in Fig. 3 and Table 4, the results comply with Salhi et al. (2017). The properties of fresh self-compacting concrete are affected by the hot weather conditions. The concrete temperature rises and the setting time of concrete decreases resulting in increasing the hydration rate at early ages. The more the decreasing setting time, the more difficult of concrete compacting.

3.2. Compressive strength

The compressive strength of self-compacting concrete in hot weather has higher values at early ages as the structure of C-S-H gel is modified in the cement, but at later ones decreased values are noticed compared to normal conditions mortar as the results obtained by Madduru et al. (2016). In hot weather, the high temperatures accelerate the hydration products causing a hydration product shell that is more dense around the clinker particles that still anhydrite (Shuai et al., 2016).

The effect of mixing water temperatures on the compressive strength of the different concrete mixes;

First, the same concrete type and different curing temperatures (25°C, 50°C):

Fig. 4 shows the relation between age and compressive strength for the (NC) and (SCC) mixes cured at 25°C, 50°C and control mix using mixing water temperature at 5°C. Fig. 4(a) illustrates that the compressive strength increases with the age. Mixes cured at 25°C and 50°C have a compressive strength slightly less than that of control mix. The compressive strength of the mixes cured at 50°C is greater than that at 25°C only at early ages (7-

days) by about 23.8%, but at later ages it was less than that at 25°C by about 9% at (28-days) and 4.6% at (56-days). That is due to the difference of concrete temperature, mixing water temperature and the surrounding temperature making cracks in concrete appear in the results at late ages. Fig. 4(b) has the same trending conditions, but the concrete type is different as the self-compacting concrete is the case of study. The results of compressive strength at (7-days) for the cured mixes at 50°C are greater than that at 25 by about 20%, less than that at 25°C by about 10% at (28-days) and less than that at 25°C by about 12% at (56-days).

Second, the same curing temperature and different concrete types (NC, SCC):

At 7-days tests, the results of self-compacting concrete specimens are always greater than conventional ones. The average compressive strength of (SCC) increased by about 1.4% compared to that of the conventional concrete. At 28-days tests, the average compressive strength of (SCC) increased by about 1.75% compared to that of the conventional concrete. At 56-days tests, the average compressive strength of (SCC) increased by about 5% compared to that of the conventional concrete.

Table 3. Shrinkage of conventional and self-compacting concrete.

Mixes	Shrinkage (%)
NC. Materials at 25°C, Mixing water at 5°C	0.049
NC. Materials at 25°C, Mixing water at 20°C	0.051
NC. Materials at 25°C, Mixing water at 35°C	0.050
SCC. Materials at 25°C, Mixing water at 5°C	0.098
SCC. Materials at 25°C, Mixing water at 20°C	0.057
SCC. Materials at 25°C, Mixing water at 35°C	0.064
NC. Materials at 50°C, Mixing water at 5°C	0.072
NC. Materials at 50°C, Mixing water at 20°C	0.049
NC. Materials at 50°C, Mixing water at 35°C	0.010
SCC. Materials at 50°C, Mixing water at 5°C	0.067
SCC. Materials at 50°C, Mixing water at 20°C	0.153
SCC. Materials at 50°C, Mixing water at 35°C	0.105
NC. Materials at 50°C, Mixing water at 35°C and using a retarder	0.067
SCC. Materials at 50°C, Mixing water at 35°C and using a retarder	0.115

Table 4. Fresh properties of self-compacting concrete.

Mixes	Slump		J-Ring		V-Funnel	
	D_{avg} (cm)	T (50cm) (sec.)	D_{avg} (cm)	H (cm)	T_o (sec.)	T (after 5mins) (sec.)
Materials at 25°C, Mixing water at 5°C	70	4.5	53	1.4	8	11
Materials at 25°C, Mixing water at 20°C	75	3.5	75	2	7	10
Materials at 25°C, Mixing water at 35°C	72	2.5	71	1.8	6	9
Materials at 50°C, Mixing water at 5°C	69	4	52	1.7	10	12
Materials at 50°C, Mixing water at 20°C	70	3	63	1.75	6.5	8.5
Materials at 50°C, Mixing water at 35°C	67	2	65	2	6	7.5
Materials at 50°C, Mixing water at 35°C and using a retarder	74	2	72	1.85	5	7

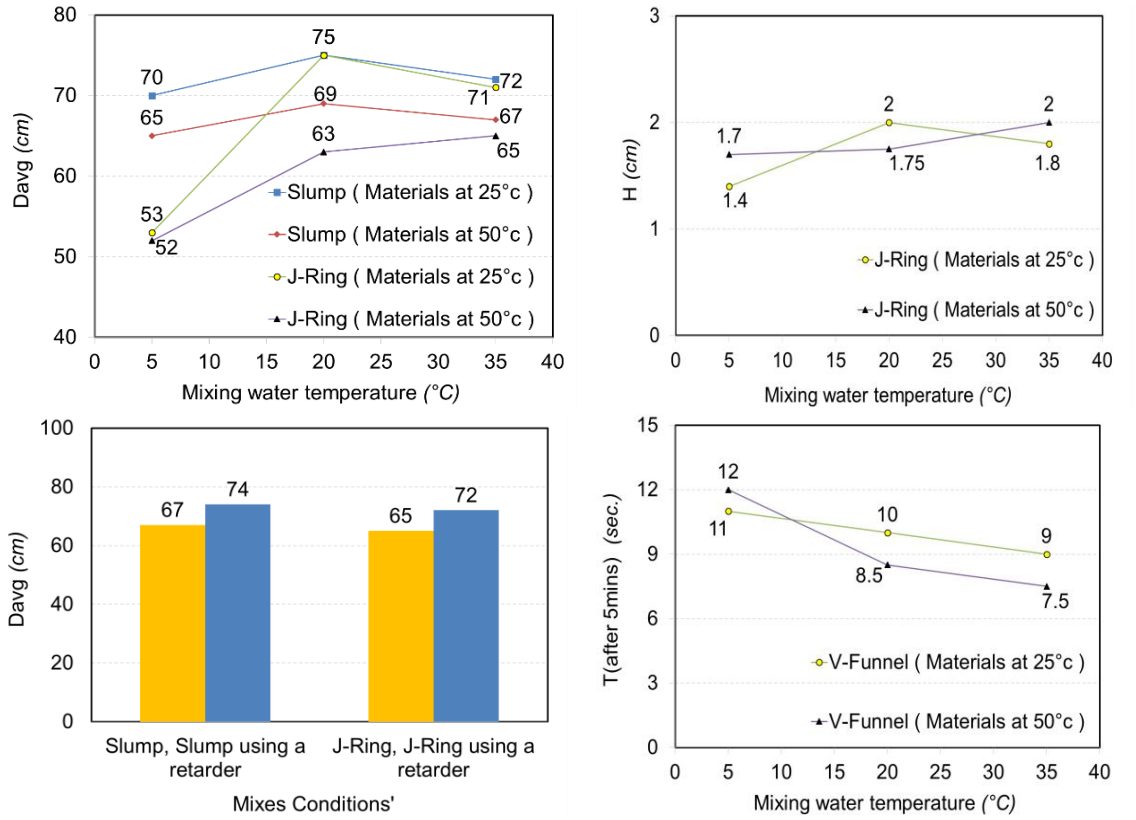

Fig. 3. Fresh properties of self-compacting concrete.

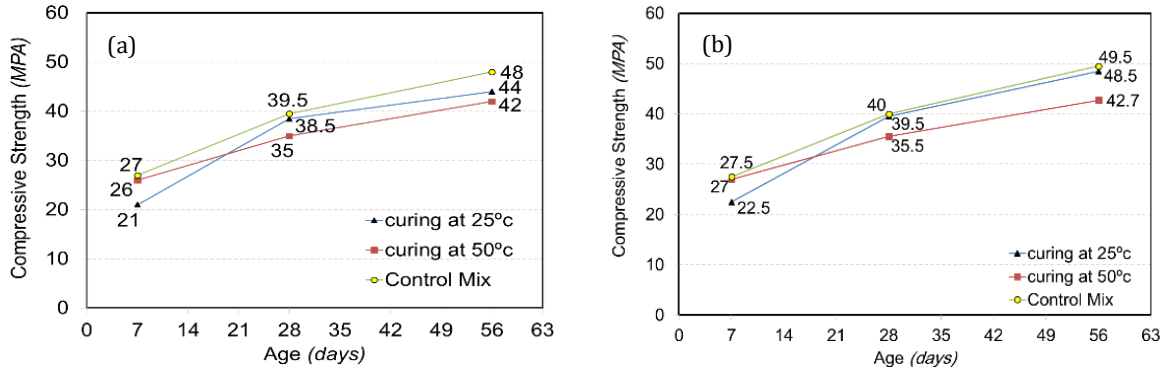

Fig. 4. Relationship between compressive strength and age using mixing materials at 25°C and mixing water at 5°C: (a) Normal concrete; (b) Self-compacting concrete.

First, the same concrete type and different curing temperatures (25°C, 50°C):

Fig. 5 shows the relation between age and compressive strength for the (NC) and (SCC) mixes cured at 25°C, 50°C and control mix using mixing water temperature at 20°C. Fig. 5(a) illustrates that the compressive strength increases with the age. Mixes cured at 25°C and 50°C have a compressive strength slightly less than that of control mix. The compressive strength of the mixes cured at 50°C is greater than that at 25°C only at early ages (7-days) by about 11%, but at later ages it was less than that at 25°C by about 5% at (28-days) and 7% at (56-days). That is due to the difference of concrete temperature, mixing water temperature and the surrounding temperature making cracks in concrete appear in the results at late ages. Fig. 5(b) has the same trending conditions, but the concrete type is different as the self-compacting concrete is the case of study. The results of compressive strength at (7-days) for the cured mixes at 50°C are greater than that at 25 by about 13%, less than that at 25°C by about 6% at (28-days) and less than that at 25°C by about 8% at (56-days).

Second, the same curing temperature and different concrete types (NC, SCC):

At 7-days tests, the results of self-compacting concrete specimens are always greater than conventional ones. The average compressive strength of (SCC) increased by about 2.63% compared to that of the conventional concrete. At 28-days tests, the average compressive strength of (SCC) increased by about 1% compared to that of the conventional concrete. At 56-days tests, the average compressive strength of (SCC) increased by about 2.7% compared to that of the conventional concrete.

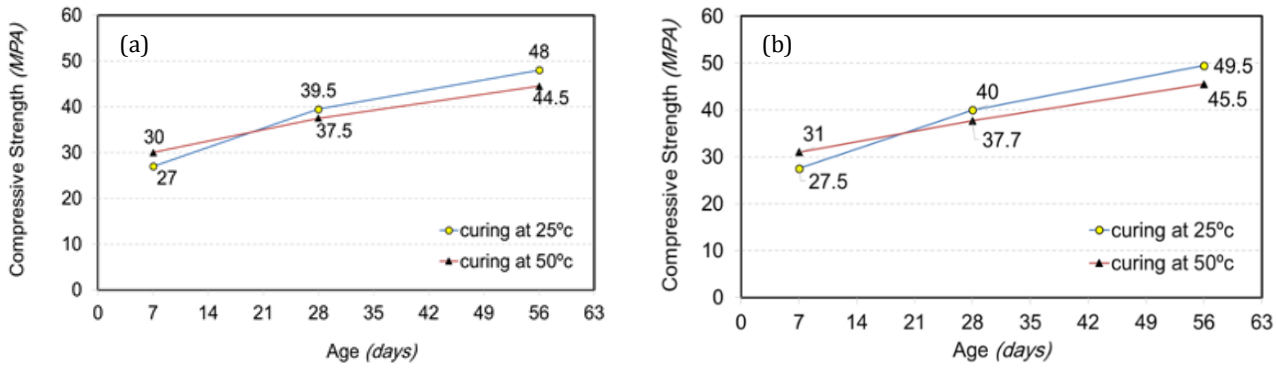

Fig. 5. Relationship between compressive strength and age using mixing materials at 25°C and mixing water at 20°C: (a) Normal concrete; (b) Self-compacting concrete.

First, the same concrete type and different curing temperatures (25°C, 50°C):

Fig. 6 shows the relation between age and compressive strength for the (NC) and (SCC) mixes cured at 25°C, 50°C and control mix using mixing water temperature at 35°C. Fig. 6(a) illustrates that the compressive strength increases with the age. Mixes cured at 25°C and 50°C have a compressive strength slightly less than that of control mix. The compressive strength of the mixes cured at 50°C is greater than that at 25°C only at early ages (7-days) by about 12%, but at later ages it was less than that at 25°C by about 13% at (28-days) and 14% at (56-days). That is due to the difference of concrete temperature, mixing water temperature and the surrounding temperature making cracks in concrete appear in the results at late ages. Fig. 6(b) has the same trending conditions, but the concrete type is different as the self-compacting concrete is the case of study. The results of compressive strength at (7-days) for the cured mixes at 50°C are greater than that at 25°C by about 10%, less than that at 25°C by about 13% at (28-days) and less than that at 25°C by about 12% at (56-days).

Second, the same curing temperature and different concrete types (NC, SCC):

At 7-days tests, the results of self-compacting concrete specimens are always greater than conventional ones. The average compressive strength of (SCC) increased by about 2.3% compared to that of the conventional concrete. At 28-days tests, the average compressive strength of (SCC) increased by about 2.25% compared to that of the conventional concrete. At 56-days tests, the average compressive strength of (SCC) increased by about 4% compared to that of the conventional concrete.

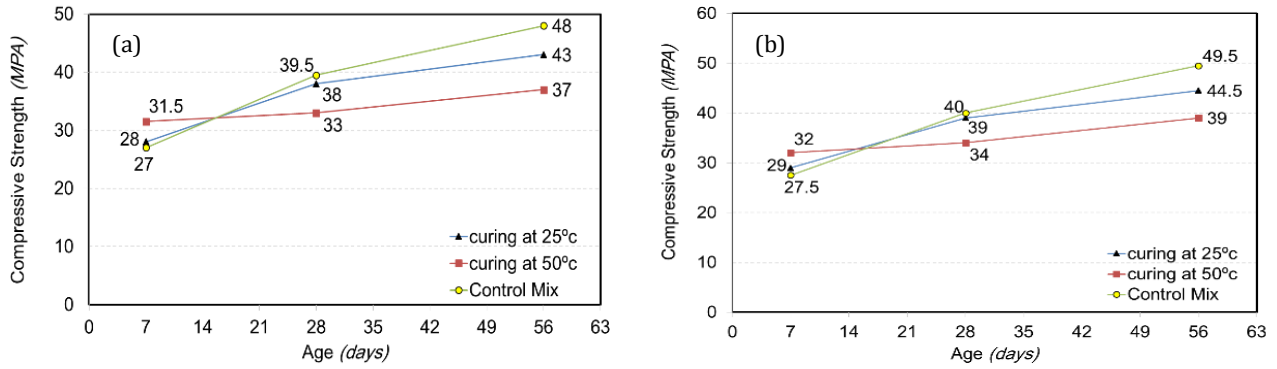

Fig. 6. Relationship between compressive strength and age using mixing materials at 25°C and mixing water at 35°C: (a) Normal concrete; (b) Self-compacting concrete.

First, the same concrete type and different curing temperatures (25°C, 50°C):

Fig. 7 shows the relation between age and compressive strength for the (NC) and (SCC) mixes cured at 25°C, 50°C and control mix using mixing water temperature at 5°C. Fig. 7(a) illustrates that the compressive strength increases with the age, mixes cured at 25°C and 50°C have a compressive strength slightly close to each other and the compressive strength of the control mix obviously is greater than other mixes. It's greater than the mixes cured at 25°C by about 237% at (7-days), 119% at (28-days) and 100% at (56-days) and also greater than mixes cured at 50°C by 145% about at (7-days), 139% at (28-days) and 113% at (56-days).

Fig. 7(b) also has the same trending conditions, but the concrete type is different as the self-compacting concrete is the case of study. The control mix is greater than the mixes cured at 25°C by about 129% at (7-days), 81% at (28-days) and 65% at (56-days) and also greater than mixes cured at 50°C by about 128% at (7-days), 100% at (28-days) and 76% at (56-days).

Second, the same curing temperature and different concrete types (NC, SCC):

At 7-days tests, the results of self-compacting concrete specimens are always greater than conventional ones. The average compressive strength of (SCC) increased by about 12% compared to that of the conventional concrete. At 28-days tests, the average compressive strength of (SCC) increased by about 10.8% compared to that of the conventional concrete. At 56-days tests, the average compressive strength of (SCC) increased by about 13.75% compared to that of the conventional concrete.

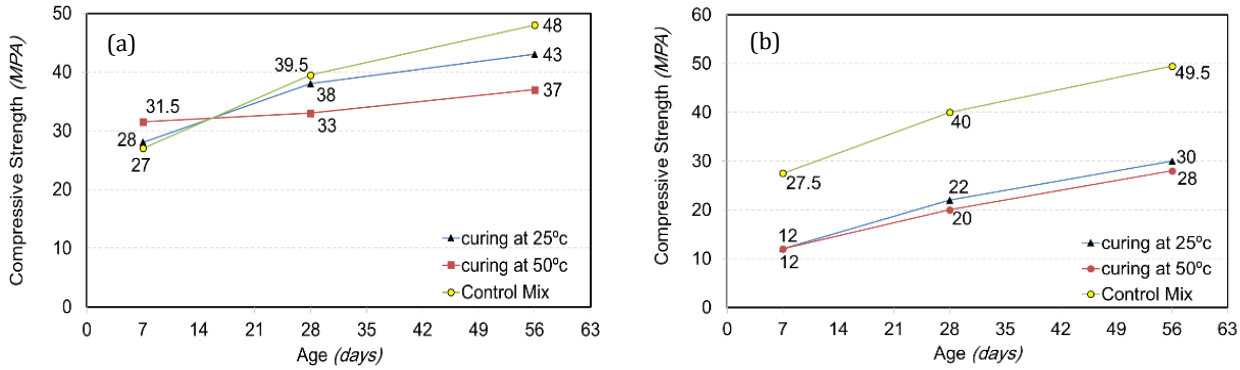

Fig. 7. Relationship between compressive strength and age using mixing materials at 50°C and mixing water at 5°C: (a) Normal concrete; (b) Self-compacting concrete.

First, the same concrete type and different curing temperatures (25°C, 50°C):

Fig. 8 shows the relation between age and compressive strength for the (NC) and (SCC) mixes cured at 25°C, 50°C and control mix using mixing water temperature at 20°C. Fig. 8(a) illustrates that the compressive strength increases with the age, mixes cured at 25°C and 50°C have a compressive strength slightly close to each other and the compressive strength of the control mix obviously is greater than other mixes. It's greater than the mixes cured at 25°C by about 200% at (7-days), 97% at (28-days) and 50% at (56-days) and also greater than mixes cured at 50°C by 125% about at (7-days), 132% at (28-days) and 62% at (56-days). Fig. 8(b) also has the same trending conditions, but the concrete type is different as the self-compacting concrete is the case of study. The control mix is greater than the mixes cured at 25°C by about 111% at (7-days), 56% at (28-days) and 35% at (56-days) and also greater than mixes cured at 50°C by about 89% at (7-days), 66% at (28-days) and 55% at (56-days).

Second, the same curing temperature and different concrete types (NC, SCC):

At 7-days tests, the results of self-compacting concrete specimens are always greater than conventional ones. The average compressive strength of (SCC) increased by about 14.6% compared to that of the conventional concrete. At 28-days tests, the average compressive strength of (SCC) increased by about 17% compared to that of the conventional concrete. At 56-days tests, the average compressive strength of (SCC) increased by about 7.8% compared to that of the conventional concrete.

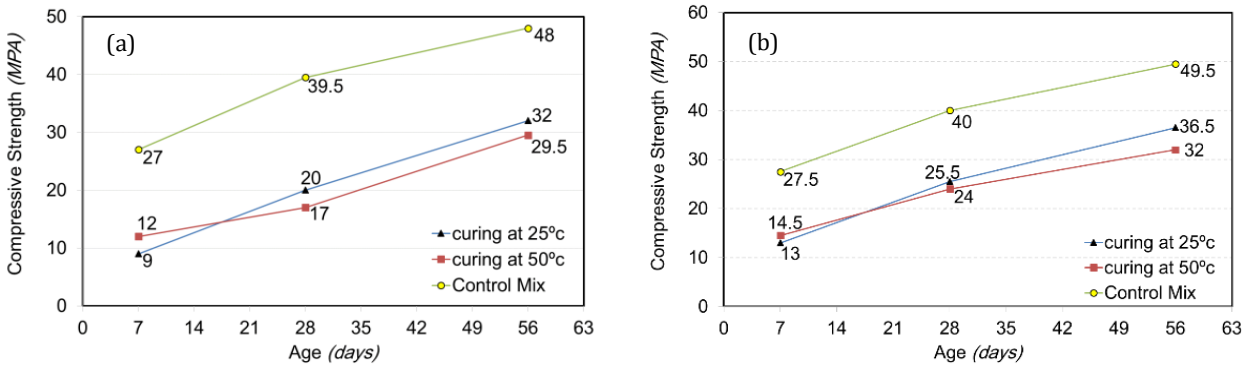

Fig. 8. Relationship between compressive strength and age using mixing materials at 50°C and mixing water at 20°C: (a) Normal concrete; (b) Self-compacting concrete.

First, the same concrete type and different curing temperatures (25°C, 50°C):

Fig. 9 shows the relation between age and compressive strength for the (NC) and (SCC) mixes cured at 25°C, 50°C and control mix using mixing water temperature at 35°C. Fig. 9(a) illustrates that the compressive strength increases with the age, mixes cured at 25°C and 50°C have a compressive strength slightly close to each other and the compressive strength of the control mix obviously is greater than other mixes. It's greater than the mixes cured at 25°C by about 134% at (7-days), 163% at (28-days) and 118% at (56-days) and also greater than mixes

cured at 50°C by 110% about at (7-days), 192% at (28-days) and 140% at (56-days). Fig. 9(b) also has the same trending conditions, but the concrete type is different as the self-compacting concrete is the case of study. The control mix is greater than the mixes cured at 25°C by about 77% at (7-days), 116% at (28-days) and 76% at (56-days) and also greater than mixes cured at 50°C by about 66% at (7-days), 128% at (28-days) and 102% at (56-days).

Second, the same curing temperature and different concrete types (NC, SCC):

At 7-days tests, the results of self-compacting concrete specimens are always greater than conventional ones. The average compressive strength of (SCC) increased by about 16% compared to that of the conventional concrete. At 28-days tests, the average compressive strength of (SCC) increased by about 11.7% compared to that of the conventional concrete. At 56-days tests, the average compressive strength of (SCC) increased by about 13.3% compared to that of the conventional concrete.

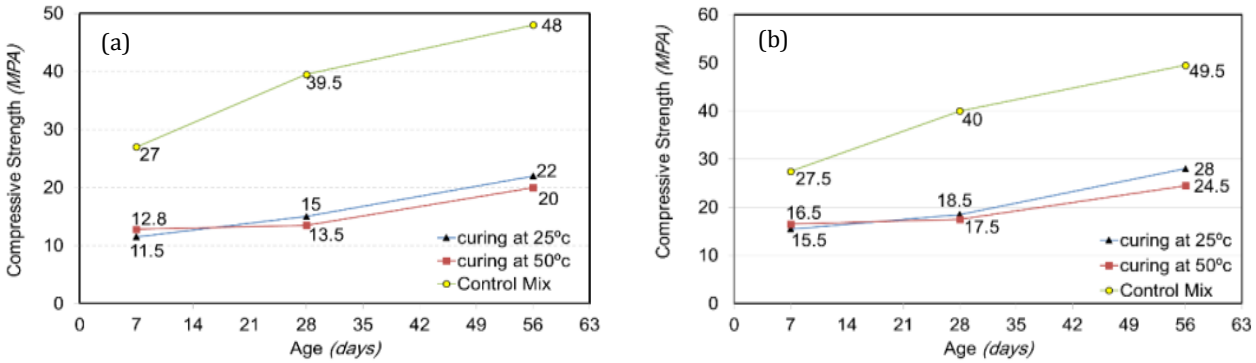

Fig. 9. Relationship between compressive strength and age using mixing materials at 50°C and mixing water at 35°C: (a) Normal concrete; (b) Self-compacting concrete.

First, the same concrete type and different curing temperatures (25°C, 50°C):

Fig. 10 shows the relation between age and compressive strength for the (NC) and (SCC) mixes cured at 50°C not using a retarder, mixes cured at 50°C using a retarder and control mix using mixing water temperature at 35°C. Fig. 10(a) illustrates that the compressive strength increases with the age, mixes cured at 50°C using a retarder have a compressive strength better than that not using a retarder and the compressive strength of the control mix obviously is greater than other mixes. It's greater than the mixes not using a retarder by about 111% at (7-days), 192% at (28-days) and 140% at (56-days) and also greater than mixes using a retarder by 92% about at (7-days), 108% at (28-days) and 118% at (56-days). Fig. 10(b) also has the same trending conditions, but the concrete type is different as the self-compacting concrete is the case of study. The control mix is greater than the mixes not using a retarder by about 66% at (7-days), 128% at (28-days) and 101% at (56-days) and also greater than mixes using a retarder by about 61% at (7-days), 81% at (28-days) and 90% at (56-days).

Second, the same curing temperature and different concrete types (NC, SCC):

At 7-days tests, the results of self-compacting concrete specimens are always greater than conventional ones. The average compressive strength of (SCC) increased by about 13% compared to that of the conventional concrete. At 28-days tests, the average compressive strength of (SCC) increased by about 10.4% compared to that of the conventional concrete. At 56-days tests, the average compressive strength of (SCC) increased by about 9.9% compared to that of the conventional concrete.

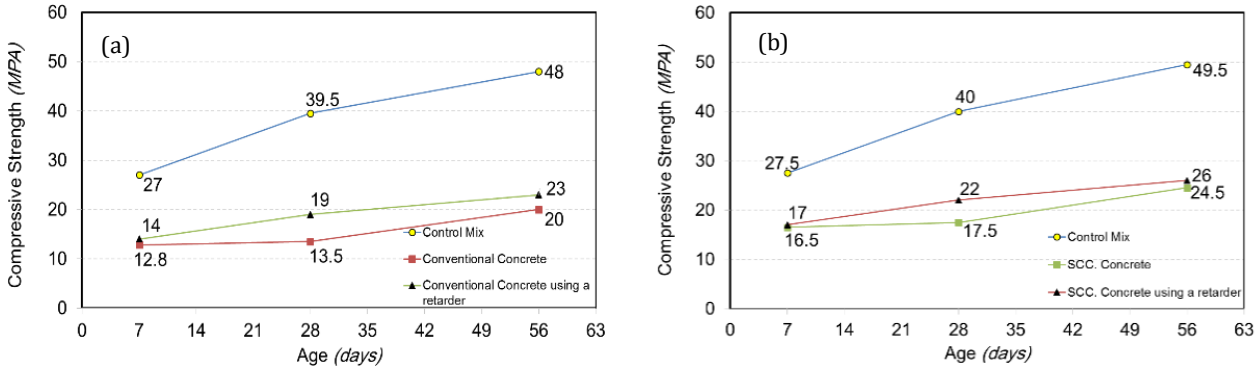

Fig. 10. Relationship between compressive strength and age using mixing materials at 50°C and mixing water at 35°C in addition to a retarder: (a) Normal concrete; (b) Self-compacting concrete.

Using a retarder had a significant effect on the results as shown in Fig. 10, there was an increase by about 9.4% and 3% for NC and SCC respectively after 7-days. After 28-days the increase was by about 40.75% and 25.71% for NC and SCC respectively. Finally, when testing after 56-days, results increased by about 15% and 6.12% for NC and SCC respectively.

3.3. Splitting tensile strength

Hot weather has the same influences of compressive strength results on splitting tensile strength results. Low tensile strength results compared to compressive strength results are also obtained. The irregular shape of crushed aggregates is very important as because of that shape water bleeding collects under the pieces of aggregates in an easy way decreasing the bond around that irregular surface and when the tensile force is applied in a zone of that irregular shape, cracks immediately develop in that zone before the other zones of concrete causing the low value of tensile strength. These results were complied with the study of (Sampebulu, 2008).

The effect of mixing water temperatures on the splitting tensile strength of the different concrete mixes;

First, the same concrete type and different curing temperatures (25°C, 50°C):

Fig. 11 shows the relation between age and splitting tensile strength for the (NC) and (SCC) mixes cured at 25°C, 50°C and control mix using mixing water temperature at 5°C. Fig. 11(a) illustrates that the splitting tensile strength increases with the age. Mixes cured at 25°C and 50°C have a splitting tensile strength slightly less than that of control mix. The splitting tensile of cured mixes at 50°C was less than that at 25°C by about 14% at (28-days) and 13% at (56-days). That is due to the difference of concrete temperature, mixing water temperature and the surrounding temperature making cracks in concrete appear in the results at late ages. Fig. 11(b) also has the same trending conditions, but the concrete type is different as the self-compacting concrete is the case of study. The results of splitting tensile strength at (28-days) for the cured mixes at 50°C, are less than that at 25°C by about 11% and by about 11.4% at (56-days). The results of self-compacting concrete specimens are always greater than conventional ones.

Second, the same curing temperature and different concrete types (NC, SCC):

The average splitting tensile strength of (SCC) control mix increased by about 3% compared to that of the conventional concrete. The average splitting tensile strength of (SCC) cured at 25°C increased by about 4.3% compared to that of the conventional concrete. The average splitting tensile strength of (SCC) cured at 50°C increased by about 7.5% compared to that of the conventional concrete.

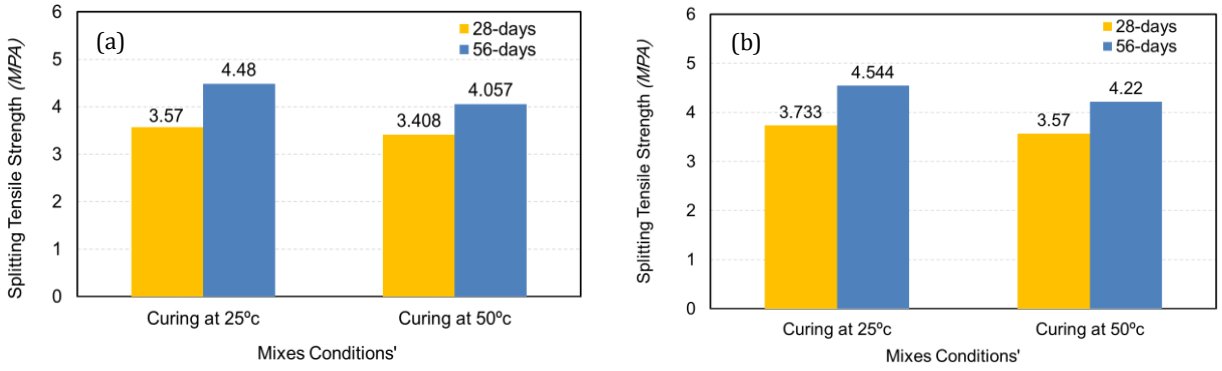

Fig. 11. Relationship between tensile strength and age using mixing materials at 25°C and mixing water at 5°C: (a) Normal concrete; (b) Self-compacting concrete.

First, the same concrete type and different curing temperatures (25°C, 50°C):

Fig. 12 shows the relation between age and splitting tensile strength for the (NC) and (SCC) mixes cured at 25°C (control mix) and cured at 50°C using mixing water temperature at 20°C. Fig. 12(a) illustrates that the splitting tensile strength increases with the age. The splitting tensile of cured mixes at 50°C was less than that at 25°C by about 4.5% at (28-days) and 9% at (56-days). That is due to the difference of concrete temperature, mixing water temperature and the surrounding temperature making cracks in concrete appear in the results at late ages. Fig. 12(b) also has the same trending conditions, but the concrete type is different as the self-compacting concrete is the case of study. The results of splitting tensile strength at (28-days) for the cured mixes at 50°C, are less than that at 25°C by about 4% and by about 7% at (56-days).

Second, the same curing temperature and different concrete types (NC, SCC):

The average splitting tensile strength of (SCC) cured at 25°C increased by about 4% compared to that of the conventional concrete. The average splitting tensile strength of (SCC) cured at 50°C increased by about 4.3% compared to that of the conventional concrete.

First, the same concrete type and different curing temperatures (25°C, 50°C):

Fig. 13 shows the relation between age and splitting tensile strength for the (NC) and (SCC) mixes cured at 25°C, 50°C and control mix using mixing water temperature at 35°C. Fig. 13(a) illustrates that the splitting tensile strength increases with the age. Mixes cured at 25°C and 50°C have a splitting tensile strength slightly less than that of control mix. The splitting tensile of cured mixes at 50°C was less than that at 25°C by about 13.2% at (28-days) and

13% at (56-days). That is due to the difference of concrete temperature, mixing water temperature and the surrounding temperature making cracks in concrete appear in the results at late ages. Fig. 13(b) also has the same trending conditions, but the concrete type is different as the self-compacting concrete is the case of study. The results of splitting tensile strength at (28-days) for the cured mixes at 50°C, are less than that at 25°C by about 17% and by about 10% at (56-days). The results of self-compacting concrete specimens are always greater than conventional ones.

Second, the same curing temperature and different concrete types (NC, SCC):

The average splitting tensile strength of (SCC) control mix increased by about 3% compared to that of the conventional concrete. The average splitting tensile strength of (SCC) cured at 25°C increased by about 8.3% compared to that of the conventional concrete. The average splitting tensile strength of (SCC) cured at 50°C increased by about 7% compared to that of the conventional concrete.

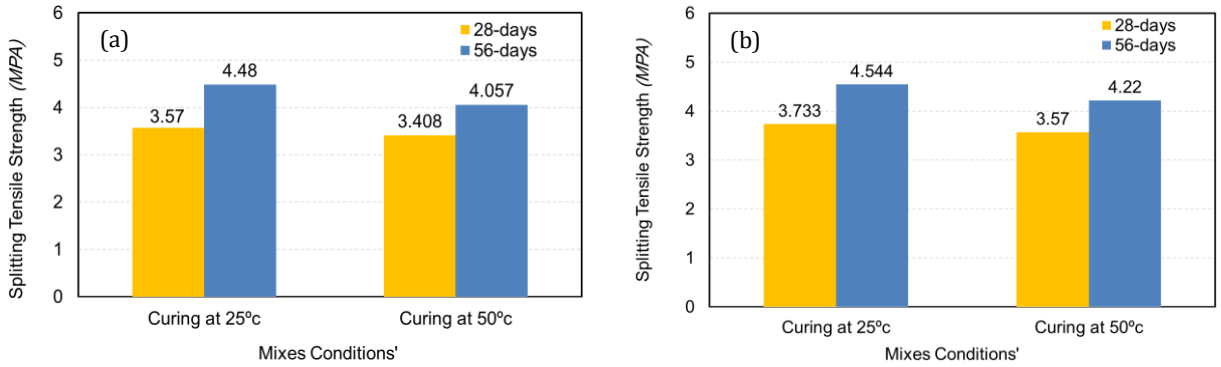

Fig. 12. Relationship between tensile strength and age using mixing materials at 25°C and mixing water at 20°C: (a) Normal concrete; (b) Self-compacting concrete.

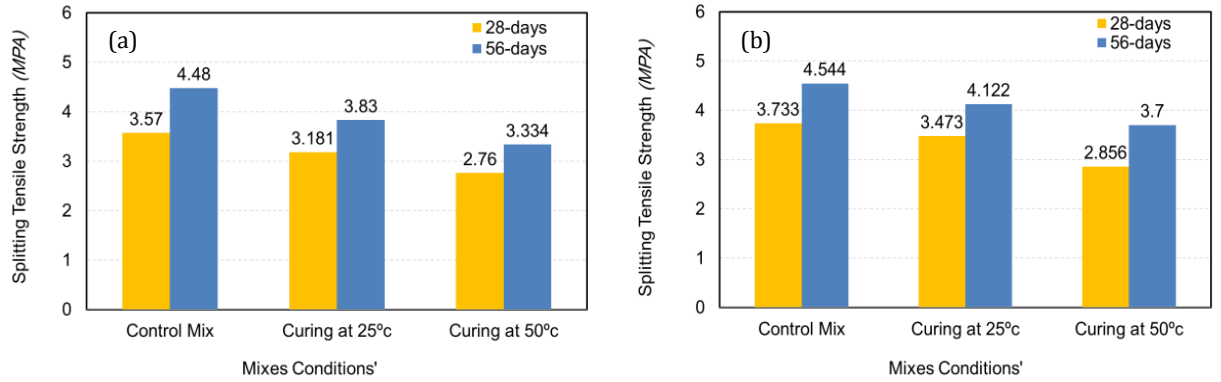

Fig. 13. Relationship between tensile strength and age using mixing materials at 25°C and mixing water at 35°C: (a) Normal concrete; (b) Self-compacting concrete.

First, the same concrete type and different curing temperatures (25°C, 50°C):

Fig. 14 shows the relation between age and splitting tensile strength for the (NC) and (SCC) mixes cured at 25°C, 50°C and control mix using mixing water temperature at 5°C. Fig. 14(a) illustrates that the splitting tensile strength increases with the age, mixes cured at 25°C and 50°C have a splitting tensile strength slightly close to each other and the splitting tensile strength of the control mix obviously is greater than other mixes. It's greater than the mixes cured at 25°C by about 42% at (28-days) and 44% at (56-days) and also greater than mixes cured at 50°C by about 83% at (28-days) and 91% at (56-days). This is due to the difference of concrete temperature, mixing water temperature and the surrounding temperature making cracks in concrete appear in the results at late ages.

Fig. 14(b) also has the same trending conditions, but the concrete type is different as the self-compacting concrete is the case of study. The control mix is greater than the mixes cured at 25°C by about 28% at (28-days) and 31% at (56-days) and also greater than mixes cured at 50°C by about 53% at (28-days) and 63% at (56-days). The results of self-compacting concrete specimens are always greater than conventional ones.

Second, the same curing temperature and different concrete types (NC, SCC):

The average splitting tensile strength of (SCC) control mix increased by about 3% compared to that of the conventional concrete. The average splitting tensile strength of (SCC) cured at 25°C increased by about 14% compared to that of the conventional concrete. The average splitting tensile strength of (SCC) cured at 50°C increased by about 22% compared to that of the conventional concrete.

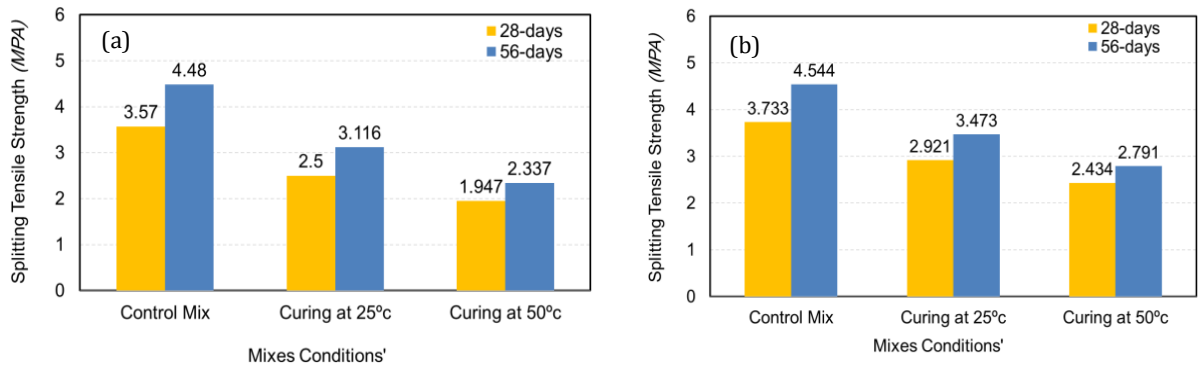

Fig. 14. Relationship between tensile strength and age using mixing materials at 50°C and mixing water at 5°C: (a) Normal concrete; (b) Self-compacting concrete.

First, the same concrete type and different curing temperatures (25°C, 50°C):

Fig. 15 shows the relation between age and splitting tensile strength for the (NC) and (SCC) mixes cured at 25°C, 50°C and control mix using mixing water temperature at 20°C. Fig. 15(a) illustrates that the splitting tensile strength increases with the age, mixes cured at 25°C and 50°C have a splitting tensile strength slightly close to each other and the splitting tensile strength of the control mix obviously is greater than other mixes. It's greater than the mixes cured at 25°C by about 25% at (28-days) and 33% at (56-days) and also greater than mixes cured at 50°C by about 65% at (28-days) and 67% at (56-days). This is due to the difference of concrete temperature, mixing water temperature and the surrounding temperature making cracks in concrete appear in the results at late ages.

Fig. 15(b) also has the same trending conditions, but the concrete type is different as the self-compacting concrete is the case of study. The control mix is greater than the mixes cured at 25°C by about 12% at (28-days) and 21% at (56-days) and also greater than mixes cured at 50°C by about 40% at (28-days) and 49% at (56-days). The results of self-compacting concrete specimens are always greater than conventional ones. The average splitting tensile strength of (SCC) control mix increased by about 3% compared to that of the conventional concrete.

Second, the same curing temperature and different concrete types (NC, SCC):

The average splitting tensile strength of (SCC) cured at 25°C increased by about 13.7% compared to that of the conventional concrete. The average splitting tensile strength of (SCC) cured at 50°C increased by about 17.8% compared to that of the conventional concrete.

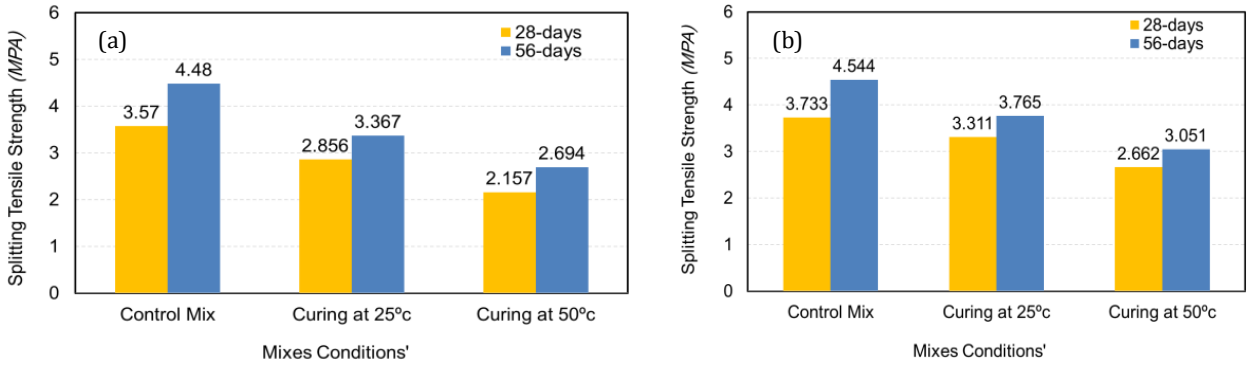

Fig. 15. Relationship between tensile strength and age using mixing materials at 50°C and mixing water at 20°C: (a) Normal concrete; (b) Self-compacting concrete.

First, the same concrete type and different curing temperatures (25°C, 50°C):

Fig. 16 shows the relation between age and splitting tensile strength for the (NC) and (SCC) mixes cured at 25°C, 50°C and control mix using mixing water temperature at 35°C. Fig. 16(a) illustrates that the splitting tensile strength increases with the age, mixes cured at 25°C and 50°C have a splitting tensile strength slightly close to each other and the splitting tensile strength of the control mix obviously is greater than other mixes. It's greater than the mixes cured at 25°C by about 57% at (28-days) and 64% at (56-days) and also greater than mixes cured at 50°C by about 100% at (28-days) and 112% at (56-days). This is due to the difference of concrete temperature, mixing water temperature and the surrounding temperature making cracks in concrete appear in the results at late ages.

Fig. 16(b) also has the same trending conditions, but the concrete type is different as the self-compacting concrete is the case of study. The control mix is greater than the mixes cured at 25°C by about 44% at (28-days) and 46% at (56-days) and also greater than mixes cured at 50°C by about 65% at (28-days) and 75% at (56-days). The results of self-compacting concrete specimens are

always greater than conventional ones. The average splitting tensile strength of (SCC) control mix increased by 3% compared to that of the conventional concrete.

Second, the same curing temperature and different concrete types (NC, SCC):

The average splitting tensile strength of (SCC) cured at 25°C increased by about 14.3% compared to that of the conventional concrete. The average splitting tensile strength of (SCC) cured at 50°C increased by about 25% compared to that of the conventional concrete.

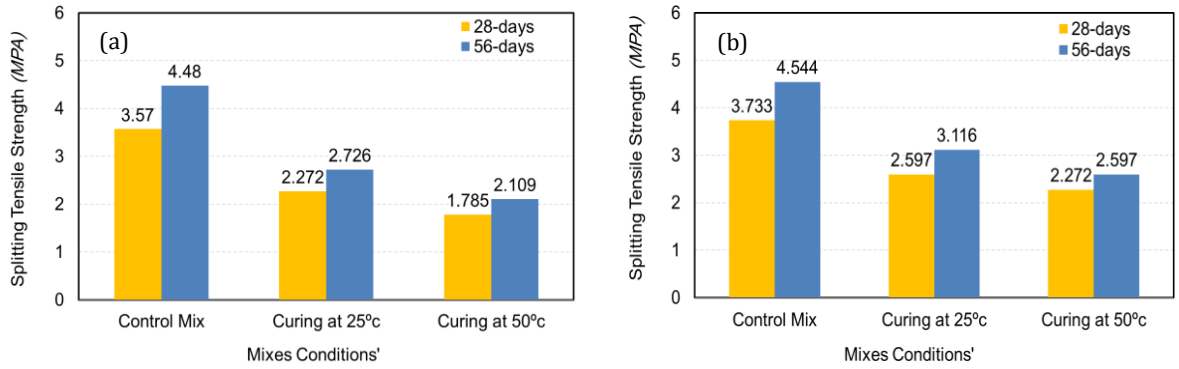

Fig. 16. Relationship between tensile strength and age using mixing materials at 50°C and mixing water at 35°C: (a) Normal concrete; (b) Self-compacting concrete.

First, the same concrete type and different curing temperatures (25°C, 50°C):

Fig. 17 shows the relation between age and splitting tensile strength for the (NC) and (SCC) mixes cured at 50°C not using a retarder, mixes cured at 50°C using a retarder and control mix using mixing water temperature at 35°C. Fig. 17(a) illustrates that the splitting tensile strength increases with the age, mixes cured at 50°C using a retarder have a splitting tensile strength better than that not using a retarder and the splitting tensile strength of the control mix obviously is greater than other mixes. It's greater than the mixes not using a retarder by about 100% at (28-days) and 112% at (56-days) and also greater than mixes using a retarder by 70% at (28-days) and 71.5% at (56-days).

Fig. 17(b) also has the same trending conditions, but the concrete type is different as the self-compacting concrete is the case of study. The control mix is greater than the mixes not using a retarder by about 66% at 64% at (28-days) and 75% at (56-days) and also greater than mixes using a retarder by about 44% at (28-days) and 56% at (56-days).

Second, the same curing temperature and different concrete types (NC, SCC):

The average splitting tensile strength of (SCC) control mix increased by about 3% compared to that of the conventional concrete. The average splitting tensile strength of (SCC) using a retarder increased by about 16.5% compared to that of the conventional concrete. The average splitting tensile strength of (SCC) cured at 50°C increased by about 25% compared to that of the conventional concrete.

Using a retarder to improve the obtained results made its job as shown in Fig. 17. There was an increase by about 18.15% for NC and 14.31% for SCC after 28-days. Also when testing after 56-days, there was an increase by about 24% for NC and 11.86% for SCC. The results of self-compacting concrete specimens are always greater than conventional ones.

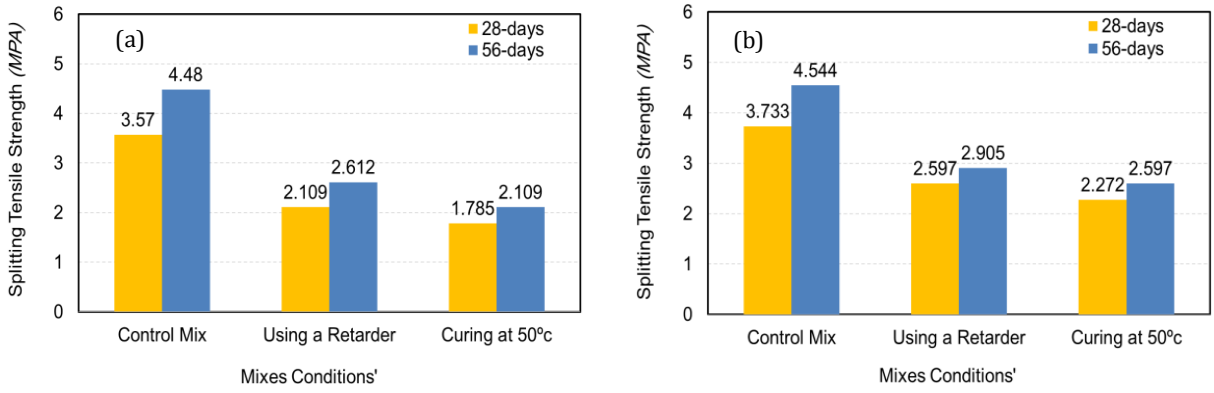

Fig. 17. Relationship between tensile strength and age using mixing materials at 50°C and mixing water at 35°C in addition to a retarder: (a) Normal concrete; (b) Self-compacting concrete.

3.4. Flexural strength

The effect of hot weather on the flexural strength of self-compacting concrete is clear as discussed in the following figures. These results comply with the work of Madi. et al. (2017).

The effect of mixing water temperatures on the flexural strength of the different concrete mixes;

First, the same concrete type and different curing temperatures (25°C, 50°C):

Fig. 18 shows the relation between mixing water temperatures and flexural strength after 28-days for the (NC) and (SCC) mixes. Fig. 18(a) shows the flexural strength results after 28-days of conventional concrete (control mix) at different mixing water temperatures. The Figure illustrates that the flexural strength increases at mixing water temperature of 20°C by 14% compared to that at 5°C. It also shows that the flexural strength decreases at mixing water temperature of 35°C by 26% compared to that at 20°C.

Fig. 18(b) shows the flexural strength results after 28-days of self-compacting concrete (control mix) at different mixing water temperatures. The figure illustrates that the flexural strength increases at mixing water temperature of 20°C by 4.7% compared to that at 5°C. It also shows that the flexural strength decreases at mixing water temperature of 35°C by 21.3% compared to that at 20°C.

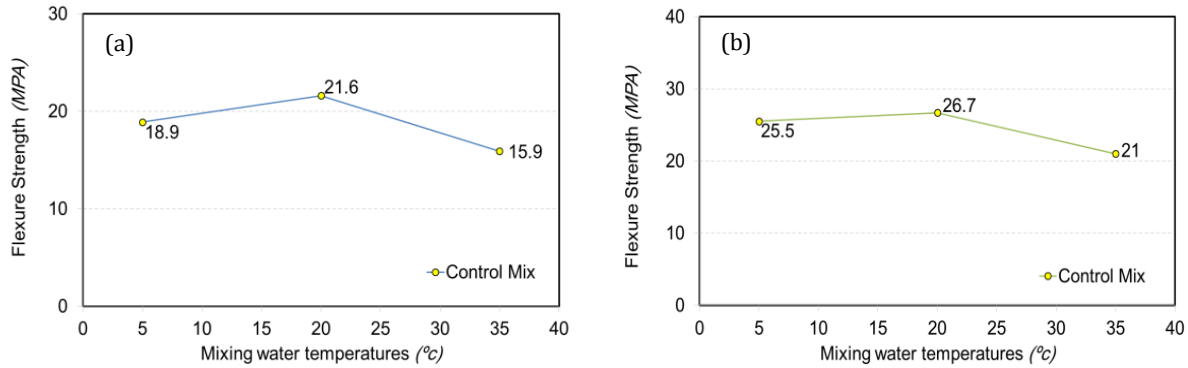

Fig. 18. Relationship between flexural strength and age using mixing materials at 25°C and mixing water at 25°C: (a) Normal concrete; (b) Self-compacting concrete.

Fig. 19 shows the relation between mixing water temperatures and flexural strength after 28-days for the (NC) and (SCC) mixes whose materials are at 25°C and cured at 50°C and control mix at different mixing water temperatures. Fig. 19(a) illustrates that the flexural strength increases at mixing water temperature of 20°C by 16.7% compared to that at 5°C. It also shows that the flexural strength decreases at mixing water temperature of 35°C by 28.6% compared to that at 20°C. The flexural strength of the control mix obviously is greater than the other mix as it's greater by about 5% at (5°C) of mixing water temperature, 3% at (20°C) and 6% at (35°C). This is due to the difference of concrete temperature, mixing water temperature and the surrounding temperature making cracks in concrete appear in the results at later ages.

Fig. 19(b) has the same trending conditions, but the concrete type is different as the self-compacting concrete is the case of study. The Figure illustrates that the flexural strength increases at mixing water temperature of 20°C by 13% compared to that at 5°C. It also shows that the flexural strength decreases at mixing water temperature of 35°C by 18% compared to that at 20°C. The control mix is greater than the other mix by about 16% (5°C), 7% at (20°C) and 3% at (35°C).

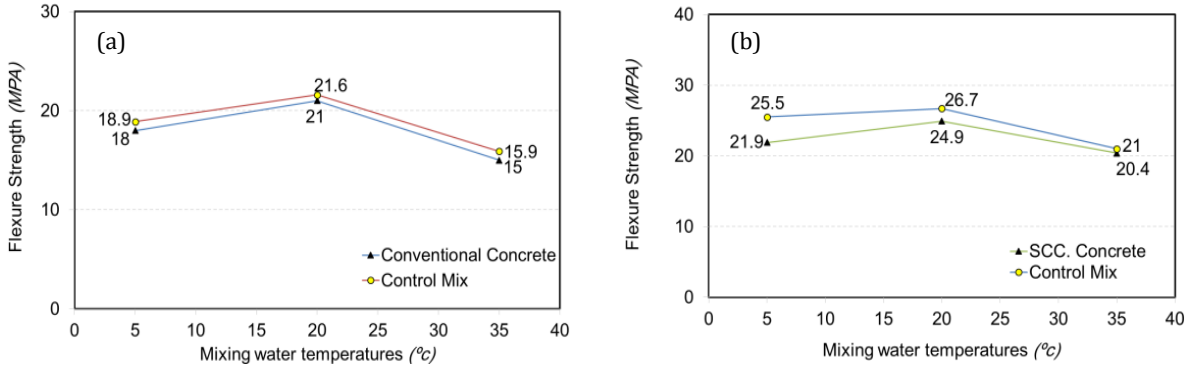

Fig. 19. Relationship between flexural strength and age using mixing materials at 25°C and mixing water at 50°C: (a) Normal concrete; (b) Self-compacting concrete.

Fig. 20 shows the relation between mixing water temperatures and flexural strength after 28-days for the (NC) and (SCC) mixes whose materials are at 50°C and cured at 25°C and control mix at different mixing water temperatures. Fig. 20(a) illustrates that the flexural strength increases at mixing water temperature of 20°C by 9% compared to that at 5°C. It also shows that the flexural strength decreases at mixing water temperature of 35°C by 12.5% compared to that at 20°C. The flexural strength of the control mix obviously is greater than the other mix as it's greater by about 43.18% at (5°C) of mixing water temperature, 50% at (20°C) and 66% at (35°C).

Fig. 20(b) also has the same trending conditions, but the concrete type is different as the self-compacting concrete is the case of study. The figure illustrates that the flexural strength increases at mixing water temperature of 20°C by 12% compared to that at 5°C. It also shows that the flexural strength decreases at mixing water temperature of 35°C by 13.3% compared to that at 20°C. The control mix is greater than the other mix by about 26.8% at (5°C), 18.7% at (20°C) and 7.7% at (35°C).

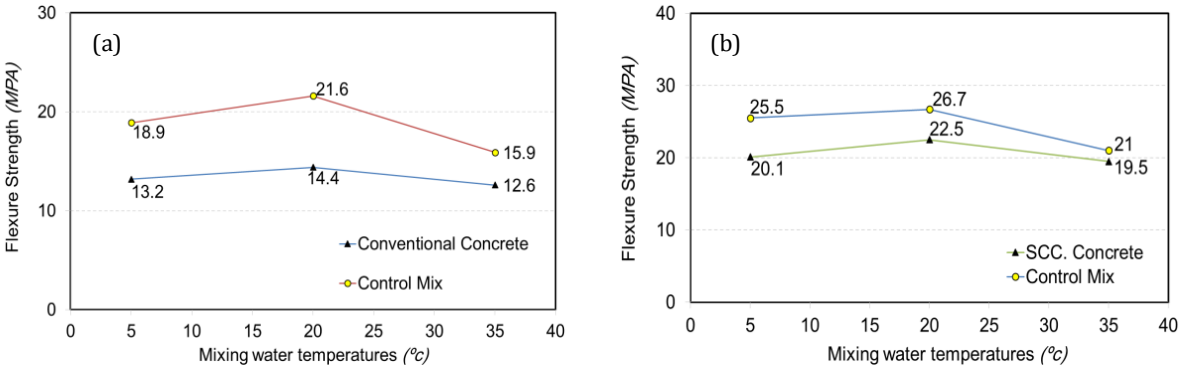

Fig. 20. Relationship between flexural strength and age using mixing materials at 50°C and mixing water at 25°C: (a) Normal concrete; (b) Self-compacting concrete.

Fig. 21 shows the relation between mixing water temperatures and flexural strength after 28-days for the (NC) and (SCC) mixes whose materials are at 50°C and cured at 50°C and control mix at different mixing water temperatures. Fig. 21(a) illustrates that the flexural strength increases at mixing water temperature of 20°C by 7.3% compared to that at 5°C. It also shows that the flexural strength decreases at mixing water temperature of 35°C by 13.6% compared to that at 20°C. The flexural strength of the control mix obviously is greater than the other mix as it's greater by about 53.7% at (5°C) of mixing water temperature, 63% at (20°C) and 39.47% at (35°C). This is due to the difference of concrete temperature, mixing water temperature and the surrounding temperature making cracks in concrete appear in the results at late ages. Fig. 21(b) also has the same trending conditions, but the concrete type is different as the self-compacting concrete is the case of study. The figure illustrates that the flexural strength increases at mixing water temperature of 20°C by 6.45% compared to that at 5°C. It also shows that the flexural strength decreases at mixing water temperature of 35°C by 16% compared to that at 20°C. The control mix is greater than the other mix by about 37% (5°C), 34.8% at (20°C) and 27.3% at (35°C).

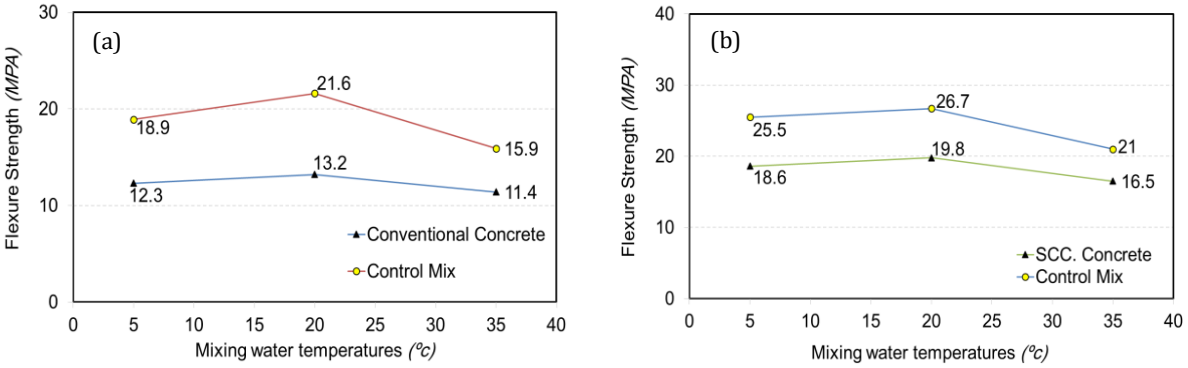

Fig. 21. Relationship between flexural strength and age using mixing materials at 50°C and mixing water at 50°C: (a) Normal concrete; (b) Self-compacting concrete.

Second, the same curing temperature and different concrete types (NC, SCC):

The previous results of flexural strength was conducted out of four stages, first one having the best results due to its ideal conditions was when the mixing materials at 25°C and the curing also at 25°C as shown in Fig. 18. Comparing the second stage (mixing materials at 25°C and the curing at 50°C) as shown in Fig. 19 to the

first stage; the flexural strength of (SCC) decreased by about 14% when mixing water was at 5°C, by about 6.75% when mixing water was at 20°C and by about 2.3% when mixing water was at 35°C, The flexural strength of (NC) decreased by about 4.7% when mixing water at 5°C, by about 2.8% when mixing water was at 20°C and by about 5.7% when mixing water was at 35°C.

Comparing the third stage (mixing materials at 50°C and the curing at 25°C) as shown in Fig. 20 to the second stage shown in Fig. 19; the flexural strength of (SCC) decreased by about 8.2% when mixing water was at 5°C, by about 9.6% when mixing water was at 20°C and by about 4.4% when mixing water was at 35°C, The flexural strength of (NC) decreased by about 2.7% when mixing water at 5°C, by about 7.6% when mixing water was at 20°C and by about 16% when mixing water was at 35°C.

Comparing the fourth stage having the worst results because of its aggressive conditions (both the mixing materials and curing at 50°C) as shown in Fig. 21 to the third stage as shown in Fig. 20; the flexural strength of (SCC) decreased by about 7.5% when mixing water was at 5°C, by about 12% when mixing water was at 20°C and by about 15.4% when mixing water was at 35°C, The flexural strength of (NC) decreased by about 6.8% when mixing water at 5°C, by about 8% when mixing water was at 20°C and by about 9.5% when mixing water was at 35°C.

Using the retarder had significant increase on the flexural strength results by about 6.78% for (NC) and 13.33% for (SCC) as shown in Fig. 22. The average flexural strength of the (SCC) is higher than that of the (NC) by 39%.

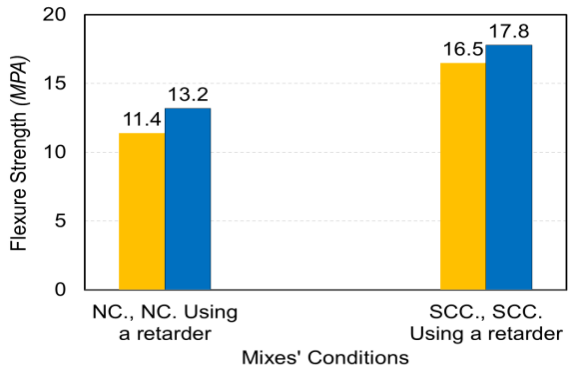

Fig. 22. Relationship between flexural strength and concrete mixes (conventional concrete and self-compacting) using mixing materials at 50°C and curing temperature of 50°C in addition to a retarder.

3.5. Concrete drying shrinkage

The curing time for concrete has a little significant effect on concrete drying shrinkage (Neville, 1996). The process of concrete drying shrinkage continues for years (Troxel et al., 1958). The results of the concrete drying shrinkage were obtained according to ASTM C157/C157M (2008). The results are shown in Table 3. There are many factors affecting the drying shrinkage which are the properties of the mixing materials, the environmental influences and the construction practices. It was found that the problem of losing moisture from the fresh concrete in hot weather because of evaporation. This problem leading to drying shrinkage cracking especially at early-ages can be minimized using shrinkage reducing admixtures (Bentz, 2006).

Studies made by Lura et al. (2011) have concluded that curing temperature plays an important role affecting the shrinkage of concrete. After 6-days of pouring, the shrinkage was 10μm/m when the curing temperature was 40°C and at 30°C, the shrinkage value was lower.

Mounanga et al. (2006) have found from their studies that shrinkage increases with temperature to a limit as when they measured it at curing temperature of 50°C was less than that at curing temperature of 40°C, they have stated that was because of structural, physical and chemical change of hydrates that are different from those measured at lower temperatures.

The tendency of both micro and macro cracks to increase occurs at elevated temperatures and this pays an important role in the increase of the total shrinkage of concrete (Maruyama and Teramoto, 2013)

The total shrinkage of concrete at curing temperature of 25 °C was more than that at curing temperature of 50 °C and that is because the potential of different reactions of cement and their relationships with cement and also the hydration mechanism (Jiang et al., 2014).

Test results showed that (SCC) concrete had better shrinkage average values compared to (NC) concrete when concrete materials were at 25°C and also when the concrete materials were at 50°C. At elevated ambient temperatures concrete shrinkage values were less than those at normal temperatures for (NC). In such hot weather conditions, concrete setting time is decreased and the hardening process occurs fast minimizing the probability of shrinkage compared to that at normal weather conditions. (SCC) shrinkage values were a little bit higher than those at normal temperatures. The retarder had a high effect increasing the shrinkage values of (NC) at hot weather while a significant increase on (SCC) shrinkage values.

4. Conclusions

The results present:

- The best performance of the two types of concrete even under high temperatures of either materials or curing are self-compacting concrete and conventional concrete respectively.
- The early curing of the specimens and covering them by burlap that also kept as wet as possible improves the properties of concrete.
- The compressive strength, splitting tensile strength and flexural strength at later ages shows that the curing compound is better than normal way of curing (water curing).
- Most un-desired results are those that were cured at 50°C and mixed of materials at 50°C, too.
- A retarder effect is very important to improve the properties of concrete especially in the most critical case of (materials temperature is at 50°C and curing temperature is also at 50°C).

The recommendations are:

- It should be clear that hot weather conditions have severe effects on both conventional and self-compacting concrete properties. As a result avoiding casting and curing at morning especially noon times in hot climates is a must.
- Using admixtures is the most helpful solution to overcome these undesired results of concrete properties.
- Types and dosages of admixtures especially retarders are the most important recommendations for any further work.
- New techniques or mixing more than a method for curing concrete in these hard conditions are also a remarkable cases of study.

Acknowledgements

All tests were carried out in the Construction Materials Laboratory in Civil Engineering Department, Faculty of Engineering, Menoufia University.

References

Ahmadi BH (2000). Initial and final setting time of concrete in hot weather. *Materials and Structures*, 33, 511-514.

Al-Amoudi OSB, Maslehuddin M, Shameem M, Ibrahim M (2007). Shrinkage of plain and silica fume cement concrete under hot weather. *Cement and Concrete Composites*, 29(9), 690-699.

Al-Feel JR, Al-Saffar NS (2009). Properties of self-compacting concrete at different curing condition and their comparison with properties of normal concrete. *Al-Rafidain Engineering Journal*, 17(3), 30-38.

ASTM C33/C33M-18 (2018). Standard Specification for Concrete Aggregates. ASTM International, West Conshohocken, PA, USA.

ASTM C157/C157M (2008). Standard Test Method for Length Change of Hardened Hydraulic-Cement Mortar and Concrete. Annual Book of ASTM Standards, Vol. 04.02 - Concrete and Aggregates, ASTM International, Conshohocken, PA, USA.

ASTM C494/C494M-17 (2017). Standard Specification for Chemical Admixtures for Concrete. ASTM International, West Conshohocken, PA, USA.

Bentz DP (2006). Influence of shrinkage reducing admixtures on early-age properties of cement pastes. *Journal of Advanced Concrete Technology*, 4(3), 423-429.

BS EN 934-2:2009+A1:2012 (2009). Admixtures for concrete, mortar and grout. Concrete admixtures. Definitions, Requirements, Conformity, Marking and Labelling.

E.C.P.203 (2017). Egyptian Code of Practice: Design and Construction for Reinforced Concrete Structures. Research Centre for Houses Building and Physical Planning, Cairo, Egypt.

E.S.S.1109 (2008). Aggregate. Ministry of Industry, Cairo, Egypt.

E.S.S.4756-1 (2012). Portland Cement, Ordinary and Rapid Hardening. Ministry of Industry, Cairo, Egypt.

EFNARC (2005). The-European-Project-Group, Specifications and guidelines for self-compacting concrete. In: European Federation of Producers and Applicators of Specialist Products for Structures.

Jiang C, Yang Y, Wang Y, Zahou Y, Ma C (2014). Autogenous shrinkage of high performance concrete containing mineral admixtures under different curing temperatures. *Construction and Building Materials*, 61, 260-269.

Lura P, Breugel K, Maruyam I (2001). Effect of curing temperature and type of cement on early-age shrinkage of high-performance concrete. *Cement and Concrete Research*, 31, 1867-1872.

Madduru SRC, Pallapothu SNRG, Pancharathi RK, Garje RK, Chakilam R (2016). Effect of self-curing chemicals in self-compacting mortars. *Construction and Building Materials*, 107, 356-364

Madi M, Refaat N, Negm El Din A, Ziada F, Mazen M, Ahmed S, et al. (2017) The impact of mixing water temperature on portland cement concrete quality. *CSCE Annual Conference*, Vancouver, Canada.

Maruyama I, Teramoto A (2013). Temperature dependence of autogenous shrinkage of silica fume cement pastes with a very low water-binder ratio. *Cement and Concrete Research*, 50, 41-50.

Mounanga P, Baroghel-Bouny V, Loukili A, Khelidj A (2006). Autogenous deformations of cement pastes: Part I. Temperatures effects at early age and micro-macro correlations. *Cement and Concrete Research*, 36, 110-122.

Mouret M, Bascoul A, Escadeillas G (2003). Strength impairment of concrete mixed in hot weather: relation to porosity of bulk fresh concrete paste and maturity. *Magazine of Concrete Research*, 55(3), 215-223.

Nasir M, Al-Amoudi OSB, Al-Gahtani HJ, Maslehuddin M (2016). Effect of casting temperature on strength and density of plain and blended cement concretes prepared and cured under hot weather conditions. *Construction and Building Materials*, 112, 529-537.

Neville AM (1996). Properties of Concrete, Fourth Edition. John Willey & Sons, Inc., New York, NY.

Park KB, Noguchi T (2017). Effects of mixing and curing temperature on the strength development and pore structure of fly ash blended mass concrete. *Advances in Materials Science and Engineering*, 2017, Article ID 3452493.

Salhi M, Ghrici M, Li A, Bilir T (2017). "Effect of curing treatments on the material properties of hardened self-compacting concrete. *Advances in Concrete Constructions*, 5(4), 359-375.

Sampebulu V (2008). Deleterious water effect on reinforced concrete used in building. *Proceeding of International Seminar on Green architecture and Environment: Towards Green Compact Cities*, Makassar, 193-202.

Shuai N, Shuguang H, Fazhou W, Pan Y, Yaohong Z, Junneng Y, Yunpeng L (2016). Internal curing: A suitable method for improving the performance of heat-cured concrete. *Construction and Building Materials*, 122, 294-301.

Troxel GE, Raphael JM, Davis RE (1958). Long-term creep and shrinkage tests of plain and reinforced concrete. *Proceedings of the ASTM*, 58, 1101-1120.